Environment International 190 (2024) 108832

Contents lists available at ScienceDirect

Environment International

journal homepage: www.elsevier.com/locate/envint

Full length article

circADAMTS6 via stabilizing CAMK2A is involved in smoking-induced emphysema through driving M2 macrophage polarization

Jiaheng Lin [a,1], Haibo Xia [a,b,1], Jinyan Yu [c,1], Yue Wang [a,1], Hailan Wang [a], Daxiao Xie [a], Cheng Cheng [a], Lu Lu [a], Tao Bian [c,*], Yan Wu [c,*], Qizhan Liu [a,*]

[a] Center for Global Health, The Key Laboratory of Modern Toxicology, Ministry of Education, School of Public Health, Suzhou Institute for Advanced Study of Public Health, Gusu School, Nanjing Medical University, Nanjing 211166, Jiangsu, People's Republic of China
[b] School of Public Health, Southeast University, Nanjing 210009, Jiangsu, People's Republic of China
[c] The Affiliated Wuxi People's Hospital of Nanjing Medical University, Department of Respiratory and Critical Care Medicine, Wuxi People's Hospital, Wuxi Medical Center, Nanjing Medical University, Wuxi 214023, Jiangsu, People's Republic of China

ARTICLE INFO

Handling Editor: Adrian Covaci

Keywords:
Emphysema
circADAMTS6
Cigarette smoke
M2 macrophage polarization

ABSTRACT

Cigarette smoke (CS), an indoor environmental pollutant, is a prominent risk factor for emphysema, which is a pathological feature of chronic obstructive pulmonary disease (COPD). Emerging function of circRNAs in immune responses and disease progression shed new light to explore the pathogenesis of emphysema. In this research, we demonstrated, by single-cell RNA sequencing (scRNAseq), that the ratio of M2 macrophages were increased in lung tissues of humans and mice with smoking-related emphysema. Further, our data showed that circADAMTS6 was associated with cigarette smoke extract (CSE)-induced M2 macrophage polarization. Mechanistically, in macrophages, circADAMTS6 stabilized CAMK2A mRNA via forming a circADAMTS6/IGF2BP2/CAMK2A RNA-protein ternary complex to activate CREB, which drives M2 macrophage polarization and leads to emphysema. In addition, in macrophages of mouse lung tissues, downregulation of circADAMTS6 reversed M2 macrophage polarization, the proteinase/anti-proteinase imbalance, and the elastin degradation, which protecting against CS-induced emphysema. Moreover, for macrophages and in a model with co-cultured lung organoids, the target of circADAMTS6 restored the growth of lung organoids compared to CSE-treated macrophages. Our results also demonstrated that, for smokers and COPD smokers, elevation of circADAMTS6 negatively correlated with lung function. Overall, this study reveals a novel mechanism for circADAMTS6-driven M2 macrophage polarization in smoking-related emphysema and postulates that circADAMTS6 could serve as a diagnostic and therapeutic marker for smoking-related emphysema.

1. Introduction

Cigarette smoke (CS), an indoor environmental pollution, contains more than 7000 chemicals, some of which constitute a serious threat to human health (Soleimani et al., 2022). Following the 2019 Global Burden of Disease study, CS affects 1.14 billion people and causes 7.69 million deaths per year (Collaborators, 2021). CS exposure is the principal environmental risk factor for the occurrence and progression of various systemic ailments, including respiratory, nervous, and cardiovascular diseases (Ma et al., 2021). Epigenetic mechanisms, including non-coding RNA, DNA modification, and histone modification, exert effects on various diseases associated with smoking (Gould, 2023). However, the specific molecular mechanisms of the adverse effects caused by smoking remain to be elucidated.

Chronic obstructive pulmonary disease (COPD) is a heterogeneous respiratory disease and a leading cause of death and disability

Abbreviations: CS, cigarette smoke; COPD, chronic obstructive pulmonary disease; scRNAseq, single-cell RNA sequencing; CSE, cigarette smoke extract; AMs, alveolar macrophages; MMP12, Matrix metallopeptidase 12; BALF, bronchoalveolar lavage fluid; ncRNAs, noncoding RNAs; CAMK2A, calcium/calmodulin-dependent protein kinase II alpha; CREB, cAMP responsive element binding protein; SPF, specific pathogen-free; TPM, total particulate matter; PMA, phorbol 12-myristate 13-acetate; GEO, Gene Expression Omnibus; TIMP1, TIMP metallopeptidase inhibitor 1; BMDMs, bone-marrow-derived macrophages; FISH, fluorescence *in situ* hybridization; ECM, Extracellular matrix; ETS, environmental tobacco smoke; SPC^{+}, surfactant protein–C–postive.

* Corresponding authors.
E-mail addresses: biantaophd@126.com (T. Bian), wuyanyangting@163.com (Y. Wu), drqzliu@hotmail.com (Q. Liu).
[1] Authors contributed equally.

https://doi.org/10.1016/j.envint.2024.108832
Received 24 January 2024; Received in revised form 8 May 2024; Accepted 17 June 2024
Available online 21 June 2024

worldwide, causing a social and economic burden (Christenson et al., 2022). Emphysema, a principal pathological feature of COPD (Hisata et al., 2021), is characterized by permanent enlargement of the distal alveolar space, attenuation of alveolar elasticity, and irreversible destruction of alveolar tissue (Vlahos, 2020). Its main pathology involves inflammation, oxidative stress, a proteinase/anti-proteinase imbalance, and apoptosis of alveolar epithelial cells (Pasupneti et al., 2020). The underlying molecular mechanisms of emphysema progression remains unclear, but is suggested to associate with imbalance of proteinases response of macrophage polarization.

Alveolar macrophages (AMs), which are mainly derived from monocytes and are abundant immune cells, contribute to respiratory disease progression via polarization into different phenotypes (Belchamber and Donnelly, 2020; Kulikauskaite and Wack, 2020). The imbalance of proteinases and their inhibitors secreted by AMs is a cause of CS-induced lung injury (Lugg et al., 2022). Matrix metallopeptidase 12 (MMP12), a macrophage-derived cytokine, is an extracellular matrix (ECM)-degrading enzyme that mediates the destruction of alveolar structures (Doyle et al., 2019). Notably, deficiency of MMP12 protected against the expansion of alveolar space and the development of emphysema in CS-exposed mice (Hautamaki et al., 1997). In addition, macrophages of the M1 phenotype, which are classically activated, produce inflammatory cytokines and kill bacteria; those of the M2 phenotype are alternatively activated and participate in immune regulation and tissue remodeling (Dong et al., 2022). Meanwhile, the clinical report showed the higher levels of M2-related genes in macrophages isolated from bronchoalveolar lavage fluid (BALF) of smokers and COPD smokers (Shaykhiev et al., 2009). However, whether M2 macrophage polarization is involved in smoking-related emphysema and the underlying molecular mechanisms need to be explored.

circRNAs, covalently closed single-stranded noncoding RNAs (ncRNAs), are generated by back-splicing from precursor mRNAs and are highly stable (Liu et al., 2021). circRNAs exhibit a diverse range of molecular mechanisms and functions in cells, and, in addition to their classical function as sponges for miRNAs, interact with proteins or mRNAs to regulate gene expression (Misir et al., 2022). In gastric cancer cells, circARID1A enhances the stability of *SLC7A5* mRNA by binding to IGF2BP3 to promote the cell proliferation (Ma et al., 2022). Diseases related to exposure to environmental chemical pollution are usually accompanied by alterations in specific circRNAs expressions (Li et al., 2020). Our previous study revealed that circRNAs are involved in CS-induced lung injury by mediating apoptosis and ferroptosis in alveolar epithelium (Xia et al., 2023; Zhao et al., 2023). circRNAs also play unique roles in immune response and regulating immune cell differentiation (Kumar et al., 2023). However, the role of circRNAs in regulating polarization of macrophage in smoking-related emphysema remains unknown.

In the present research, we establish the mechanism for circADAMTS6-driven M2 macrophage polarization in smoking-related emphysema. Mechanically, circADAMTS6 recruits IGF2BP2 to stabilize calcium/calmodulin-dependent protein kinase II alpha (CAMK2A) mRNA via forming a circADAMTS6/IGF2BP2/CAMK2A RNA-protein ternary complex, which activates cAMP responsive element binding protein (CREB), a transcription factor, to promote M2 macrophage polarization. M2 macrophages trigger a proteinase/anti-proteinase imbalance and cause elastin degradation, which contributes to the destruction of the alveolar structure, leading to emphysema. Herein, we demonstrate that circADAMTS6 is involved in CS-induced emphysema via driving M2 macrophage polarization, and circADAMTS6-driven M2 polarization is a potential target for smoking-related emphysema.

2. Methods

2.1. Human samples

Lung tissues of humans used in this study were collected from lobectomies for benign lung nodules or from lung transplants performed at Wuxi People's Hospital affiliated to Nanjing Medical University (NJMU). The protocol for human research was approved by the ethics committee of NJMU (number: 2021-130). All human samples were obtained with informed consent from human donors and were anonymized before use. Physician diagnoses of COPD followed Global Strategy for Diagnosis, Treatment, and Management of COPD. For qRT-PCR, a cohort of serum samples were harvested from COPD smokers, Smokers, and Non-smokers. The clinicopathological characteristics for serum donors and for lung tissue donors are collected in Tables 1 and S1.

2.2. Mice with CS-induced emphysema

Male BALB/c mice at 6 weeks of age, obtained from the Animal Core Facility of NJUM, were housed under specific pathogen-free (SPF) conditions at the Safety Assessment and Research Center for Drug, Pesticide and Veterinary Drug of Jiangsu Province. The protocols for animals were reviewed and approved by the animal ethics committee of NJUM (IACUC-2209016, IACUC-2209049).

Mice were housed in an SPF room, maintained at a constant temperature (23 ± 3 °C), relative humidity (40 %–70 %), and with successive 12-hr light/dark cycles. Based on the existing research and our previous study, we established the concentration of CS to be used in mice and established mice with CS-induced emphysema. Yoshida et al. induced experimental COPD in mice at 6–8 weeks of age by using a whole-body exposure system, which exposed them to CS (200 mg/m^3 total suspended particles) from 3R4F Research Cigarettes five days a week for six months (Yoshida et al., 2019). Ten mice were exposed to five 3R4F reference cigarettes at 30-min smoke-free intervals four times a day, five days a week for 24 weeks, and lungs of the mice showed expansion of alveolar space and destruction of alveolar walls (Bracke et al., 2013). Our previous study showed that mice with CS-induced emphysema were exposed to 300 mg/m^3 total particulate matter (TPM) in a whole-body exposure system for 60 min twice a day, 4 h apart, 5 days a week for a total of 16 weeks (Xia et al., 2022; Zhao et al., 2023). Further, we converted environmental tobacco smoke (ETS) exposure dose for humans and mice based on published ETS exposure dose conversion models (Hartog et al., 2019; Phillips, 2017). The CS exposure dose of 0, 200, and 300 mg/m^3 in mice is equivalent to none, moderate (0.5–1 pack/day), and severe smoking (>1 pack/day) for humans (Jang et al., 2012). In the present study, the exposure protocol for a mouse model of emphysema was as previously reported (Xia et al., 2023). In brief, mice were placed in a whole-body exposure system (Beijing Huironghe Technology CO., Ltd., China) and exposed at 200 or 300 mg/m^3 TPM using 3R4F Research Cigarettes from the University of Kentucky, USA. The mice were chronically exposed to CS for 1 hr twice a day, with smoke-free intervals of 4 hr, five days a week for 24 weeks. Age-matched mice kept in a similar environment without exposure to CS served as controls. Finally, with this concentration of CS, there was destruction of the alveolar wall and an increase in the mean linear intercept in the mouse lungs, which was involved in the progression of

Table 1
Clinical information for human serum donors.

	Non-smokers	Smokers	COPD smokers
Number	35	28	40
Sex (male)	33 (94.3 %)	27 (96.4 %)	37 (92.5 %)
Age (years)	60.5 ± 5.8	63.6 ± 7.2	65.6 ± 7.4
BMI	25.4 ± 2.8	24.6 ± 3.1	23.3 ± 4.4
Smoking history (pack-years)	–	31.3 ± 15.7	45.9 ± 33.3
GOLD grade, I/II/III/IV	–	–	12/11/10/7
FEV_1 (%) predicted	92.7 ± 14.5	85.5 ± 16.7	58.5 ± 25.2$^{**,\#\#}$
FEV_1/FVC (%)	82.9 ± 7.0	82.7 ± 7.8	52.1 ± 12.3$^{**,\#\#}$

Data are presented as means ± SD.
** $P < 0.01$ versus Non-smokers group.
$^{\#\#}$ $P < 0.01$ versus Smokers group.

smoking-related emphysema (Fig. S1).

2.3. Cell culture

THP-1 cells and RAW264.7 cells were obtained from the Shanghai Institute of Cell Biology, Chinese Academy of Sciences. THP-1 cells were maintained in RPMI-1640 (Life Technologies/Gibco, C11875500BT), and RAW264.7 cells were maintained in Dulbecco's modified Eagle's medium (Life Technologies/Gibco, C11875500BT) containing 10 % fetal bovine serum (FBS, Life Technologies/Gibco, 10099141C) and 0.1 % Penicillin-Streptomycin (Beyotime Institute of Biotechnology, C0222) under 5 % CO_2 at 37 °C. THP-1 monocytes were treated with 100 μg/mL of phorbol 12-myristate 13-acetate (PMA, Sigma-Aldrich, St. Louis, MO) for 48 h to transform them into macrophage-like cells, THP-Ms. This was followed by removing the PMA by washing and a 24-hr rest period in fresh media prior to treatment. PMA (10 mg/mL) was dissolved in DMSO to 1 mg/mL, then diluted to 100 μg/mL in RPMI-1640. Aliquots were stored at −80 °C. The THP-1 cells were passaged at a ratio 1:2 every 2 days. The RAW264.7 cells were passaged at a ratio 1:4 every 2 days.

Bone-marrow-derived macrophages (BMDMs) were extracted with the following protocol (Tang et al., 2022a). First, male BALB/c mice were sacrificed at 12 weeks of age under permission of the animal ethics committee of NJMU. Mice were immersed in iodophor, and femurs and tibias were removed on a clean laboratory bench. All bones were transferred to 75 % ethanol for disinfection and kept in ice-cold sterile PBS. Second, the bones were flushed with ice-cold PBS by suction in a 1-mL syringe until the color was white. The collected cell suspension was filtered through a 0.70-μm pore filter, and the suspension was centrifuged at 1500 rpm for 5 min. Cells were suspended in 1 mL of red blood cells lysis buffer (Solarbio, R1010) for 5 min, and the cell suspension was centrifuged at 1500 rpm for 5 min. The bone marrow cells were maintained in Dulbecco's modified Eagle's medium (Life Technologies/Gibco, C11875500BT) containing 20 % fetal bovine serum (FBS, Life Technologies/Gibco, 10099141C), 0.1 % Penicillin-Streptomycin (Beyotime, C0222), and 20 ng/ml M-CSF (PeproTech, 315-02) under 5 % CO2 at 37 °C for 7 days. The purity of the BMDM culture was validated by flow cytometry; the percentage of $F4/80^+$ cells was >90 % (Fig. S7A).

According to previous research and the association of the exposure dose between humans and cell cultures, we identified the concentration of CS used in cell culture. As previously reported, Fu et al. induced M2 macrophage polarization by treatment with 0.25 %, 0.5 %, 1 %, 2 %, or 4 % CSE (Fu et al., 2015). Our previous study showed that 1 %, 2 %, and 4 % CSE promotes the progression of Non-Small Cell Lung Cancer by inducing M2 polarization of macrophages *in vitro* (Cheng et al., 2023). In our study, there was an increased number of M2 macrophages in CSE-treated macrophage cell lines and primary macrophages with a dose–response relationship (Figs. S7B and 8A). In addition, 2.5 % to 10 % CSE roughly corresponds to exposure from smoking 0.5 to 2 packs of cigarettes per day (Su et al., 1998). Referring to relevant studies, the concentrations of 0 %, 1 %, 2 %, and 4 % CSE for macrophages is similar to none, mild (0.5 pack/day), moderate (0.5–1 pack/day), and severe smoking (>1 pack/day) by humans (Jang et al., 2012). Therefore, we treated macrophages with 0 %, 1 %, 2 %, or 4 % CSE.

2.4. Silencing of circADAMTS6 in macrophages of mouse lung tissue

AAV9-circADAMTS6 shRNA was purchased from VigeneBio (Shangdong, China). pAV-F4/80-GFP-mir30.shRNA with an inserted nonsense sequence was used as a negative control. We administered 100 μL of sterile saline containing 5×10^{11} virus particles by a nasal drip once a week for two weeks, initiating treatment after a week of CS exposure. Animals were checked daily, and their weights were compared to those for control mice. The viral load in the lungs of the mice peaked from 2 weeks to 1 month, after which the efficiency of infection was verified by fluorescence.

2.5. Statistical analysis

Statistical analyses were performed by use of GraphPad Prism 9 (Graphpad Software Inc., San Diego, CA) or SPSS 19.2 (SPSS Inc., Chicago, USA). Data were derived for at least three independent experiments and were presented as means ± SD or SEM. Methods of statistical testing included unpaired Student's t tests, chi-square tests, and one-way analysis of variance with Bonferroni correction. For the human population, the Pearson correlation coefficient was used to assess the correlation between serum circADAMTS6 expression and lung function. The differences were statistically significant when $P < 0.05$ or $P < 0.01$.

Further details of materials and methods are described in supplementary information.

3. Results

3.1. M2 macrophage polarization exists in smoking-related emphysema

Emphysema is a common characteristic of COPD (Spix et al., 2022). To elucidate the macrophage phenotype in smoking-related emphysema, we analyzed the results of scRNAseq from GSE173896 and GSE168299. These results were validated for both human and mouse lung tissues by immunofluorescent staining and western blotting (Fig. 1A). We identified 16 cell lineages, which expressed specific marker genes, from 3 normal and 5 COPD patients by dimensionality reduction and cluster analysis (Fig. 1B and 1C). Then, we proceeded to recluster the macrophages using the UMAP analysis and formed 7 cell lineages (Fig. 1D and 1E). The ratio of M2 macrophages was increased in COPD lungs, compared to the control lungs (Fig. 1F). In addition, we also analyzed scRNAseq from GSE168299 and identified 18 cell lineages on mouse lung tissues treated with or without CS (Fig. 1G and 1H). Macrophages were reclustered into 3 cell lineages and the ratio of M2 macrophages was elevated in lungs of mice exposed to CS (Fig. 1I–K). Previous studies have shown that AMs of the M2 phenotype were elevated in BALF of normal smokers and COPD patients, which is consistent with results in CS-exposed COPD mouse models (Eapen et al., 2017; He et al., 2017). Then, we collected lung tissues from COPD smokers, Smokers, and Non-smokers (Table S1) and established mice with CS-induced emphysema (Fig. S1A and S1B). The numbers of $CD68^+CD206^+$ M2 macrophages were elevated for Smokers and COPD smokers (Fig. 2A). We evaluated the M2 macrophage polarization in the lungs of COPD patients following the GOLD guideline and found that the numbers of $CD68^+CD206^+$ cells were elevated with the development of COPD (Fig. S2). The protein levels of ARG1 were also elevated (Fig. 2B). In addition, as determined by RNA-seq, there was elevated expression of M2 genes of AMs from Smokers and COPD smokers as shown by data from two Gene Expression Omnibus (GEO) databases (GSE13896 and 130928) (Fig. S3). In lung tissues of mice, the numbers of $F4/80^+CD206^+$ M2 macrophages were elevated (Fig. 2E), as were ARG1 protein levels (Fig. 2F). These findings demonstrate that M2 macrophages are elevated in smoking-related emphysema.

The imbalance of proteinase/anti-proteinase derived from macrophages is the central mechanism of COPD pathogenesis (Ishii et al., 2014). We found that, in Smokers and COPD smokers, the numbers of $MMP12^+$ cells in $CD206^+$ M2 macrophages, which degrades elastin, was elevated (Fig. 2C). In the lung tissues of humans, MMP12 protein levels were elevated, but TIMP metallopeptidase inhibitor 1 (TIMP1), which is involved in controlling MMP12 activity (Spix et al., 2022), protein levels were lower (Fig. 2D). In addition, as determined with the two GEO databases described above, MMP12 expressions were increased and TIMP1 expressions were decreased in AMs from smokers and COPD smokers (Fig. S4). The protein levels of elastin decreased in Smokers and COPD smokers (Fig. 2D). Further, we found the same effects in CS-induced lungs of mice (Fig. 2G and 2H). Together, these results show that a proteinase/anti-proteinase imbalance and elastin degradation, induced by M2 macrophage polarization, exist in smoking-related

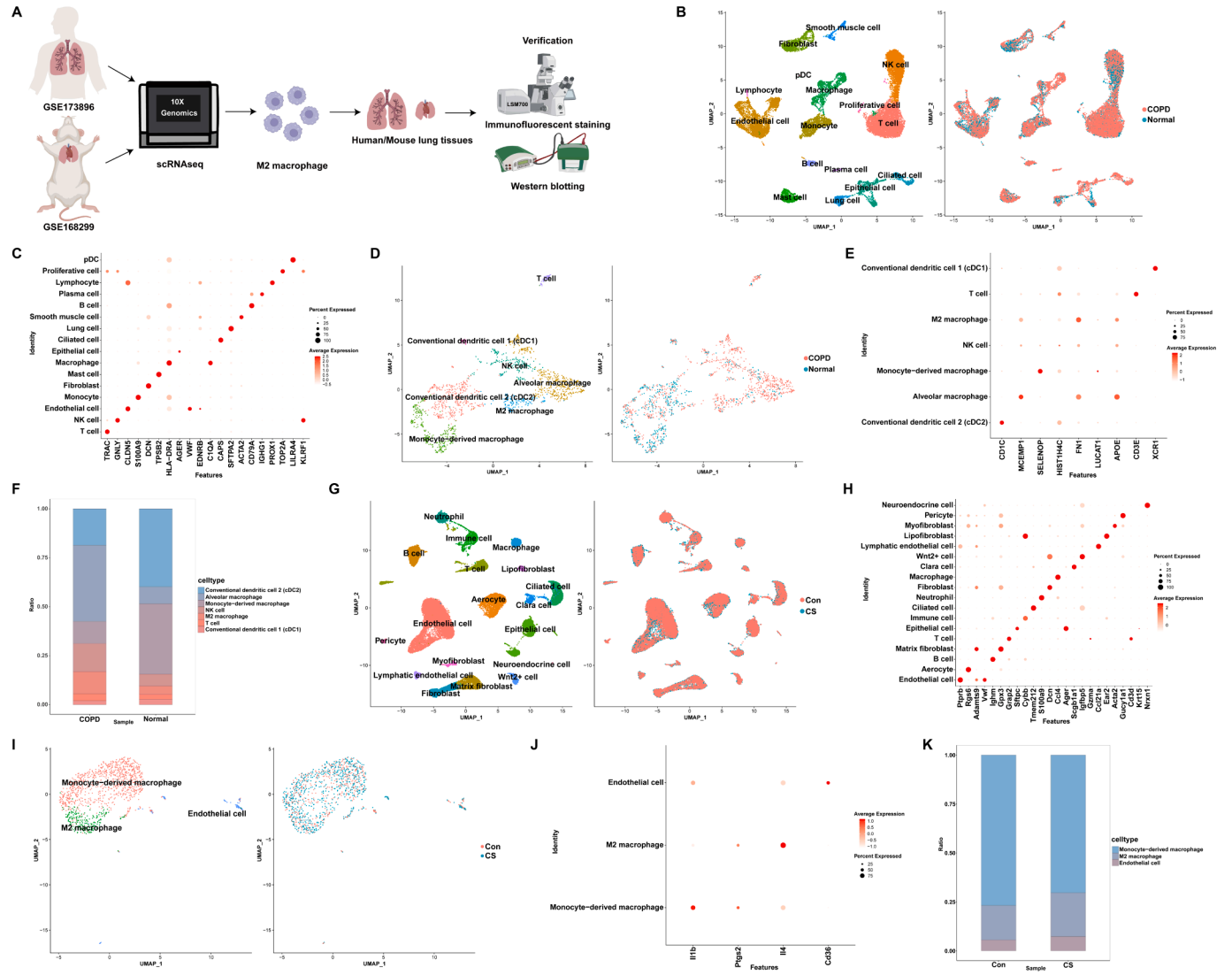

Fig. 1. Single-cell transcriptomic atlas of lung cells and macrophages in lung tissues of human and mice. (A) Schematic chart of workflow. The results of scRNAseq from GSE173896 and GSE168299 showed expression of M2 macrophage in lung tissues, which were validated for human and mouse lung tissues by immunofluorescent staining and western blotting. (B) Uniform manifold approximation and projection (UMAP) visualizing the distribution of identified 16 lung cell lineages from 3 normal and 5 COPD patients (GSE173896). (C) Dot plots showing the expression of marker genes for per-cell cluster. (D) UMAP analysis of macrophages identified 7 distinct clusters. (E) Dot plots showing the expression of marker genes for per-cell cluster. (F) The ratio of different cell lineages in macrophages, colored by cell lineages. (G) Uniform manifold approximation and projection (UMAP) visualizing the distribution of identified 18 lung cell lineages from 4 mice treated without CS and 4 mice treated with CS (GSE168299). (H) Dot plots showing the expression of marker genes for per-cell cluster. (I) UMAP analysis of macrophages identified 3 distinct clusters. (J) Dot plots showing the expression of marker genes for per-cell cluster. (K) The ratio of different cell lineages in macrophages, colored by cell lineages.

emphysema.

3.2. *The levels of circADAMTS6 are elevated in CSE-treated macrophages*

To explore the role of circRNAs in macrophages, we utilized macrophages (THP-Ms) derived from THP-1 cells and BMDMs. Firstly, we performed circRNA sequencing for THP-Ms exposed to 0 % or 4 % CSE, and found 45 altered circRNAs ($P < 0.05$ and $|\log^2 FC| > 2.0$) compared to controls as shown by a heatmap (Fig. 3A). A volcano plot (Fig. 3B) showed the top ten up-regulated circRNAs, which are circ_0007113 (circHERC4), circ_0072688 (circADAMTS6), circ_0001821 (circPVT1), circ_0003836 (circUGGT2), circ_0008338 (circZNF215), circ_0000033 (circCEP85), circ_0006063 (circAPBB1IP), circ_0004851 (circCAPRIN1), circ_0008043 (circPTGR1), and circ_0016374 (circTFEC). Subsequently, the levels of the top ten up-regulated circRNAs in THP-Ms were determined by qRT-PCR (Fig. 3C) or in BMDMs (Fig. S5) exposed to 0 %, 1 %, 2 %, or 4 % CSE for 48 h. In CSE-treated macrophages, circADAMTS6 and circAPBB1IP were elevated in a concentration-dependent manner, but circADAMTS6 was most significantly increased (Fig. 3C and S5). Based on these results, circADAMTS6 was selected for further validation and for functional experiments.

circADAMTS6 was formed by back-splicing of exon 2–7 of the ADAMTS6 gene in THP-Ms and BMDMs (Fig. 3D). Divergent primers that amplify circADAMTS6 detected only in cDNA but not in gDNA, and circADAMTS6 amplified from cDNA, were resistant to RNase R (Fig. 3E). The expression of circADAMTS6 was more stable than linear ADAMTS6 mRNA (Fig. 3F). Furthermore, circADAMTS6 was localized principally in the cytoplasm of THP-Ms, as demonstrated by nuclear and cytoplasmic extraction (Fig. 3G) and fluorescence *in situ* hybridization (FISH) (Fig. 3H) examinations. Finally, by use of FISH and immunofluorescence assays, we found that, in lung tissues of Smokers and COPD smokers, the expression of circADAMTS6 was elevated and mainly

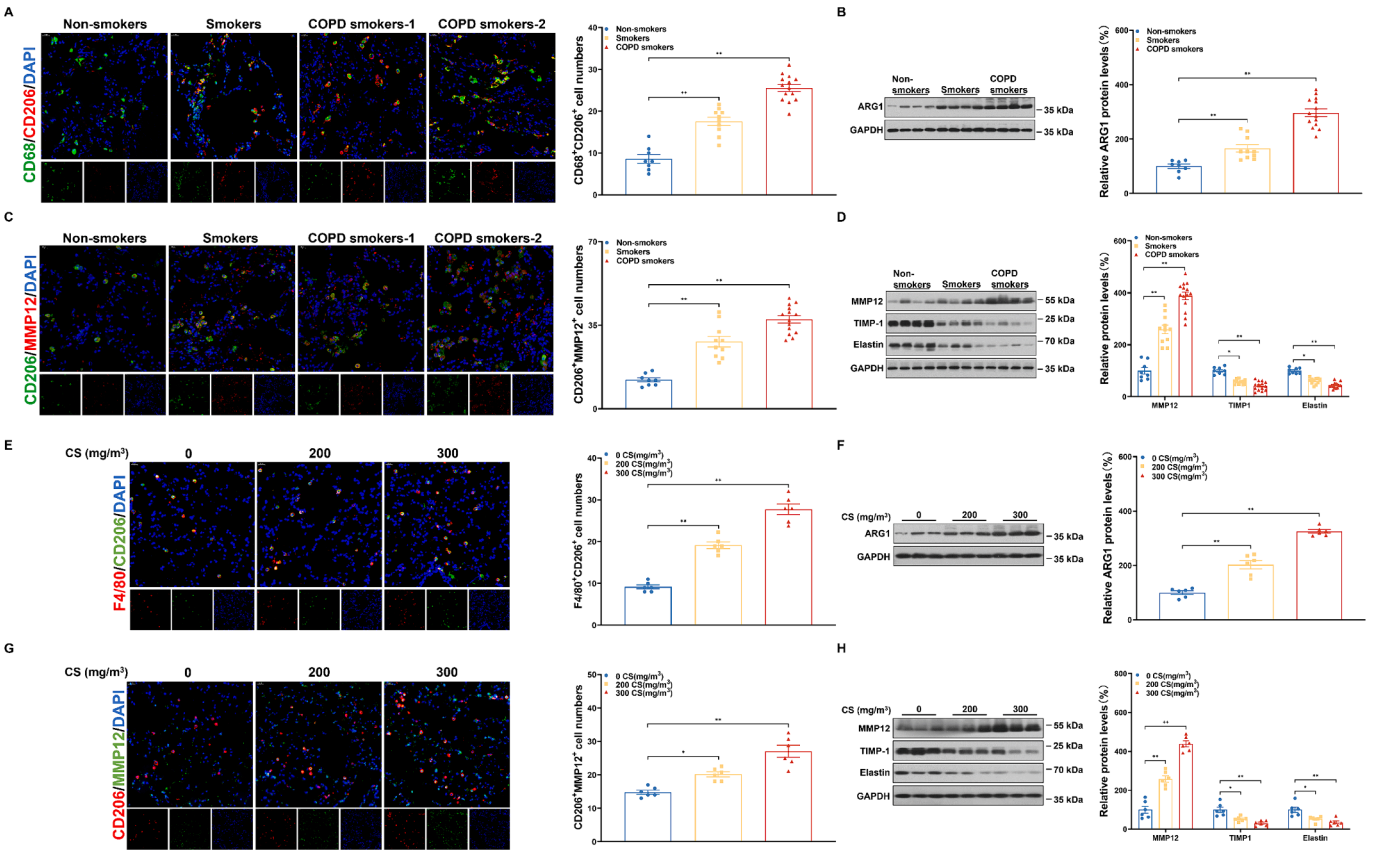

Fig. 2. M2 macrophages, a proteinase/anti-proteinase imbalance and the degradation of elastin exist in smoking-related COPD and in mice with CS-induced emphysema. Lung tissues of humans were collected from Non-smokers (n = 8), Smokers (n = 10), or COPD smokers (n = 14). Male BALB/c mice (n = 6) at 6 weeks of age were exposed to 0, 200, or 300 mg/m^3 TPM CS for 24 weeks. (A) Representative images (left) of CD68 and CD206 immunostaining in lung tissues of humans (scale bars, 20 μm). The numbers of CD68$^+$CD206$^+$ cells in lung tissues of human (right). (B) Representative immunoblots (left), and relative quantitative expressions (right) of ARG1 in lung tissues of human. (C) Representative images (left) of CD206 and MMP12 immunostaining of lung tissues of humans (scale bars, 20 μm). The numbers of CD206$^+$MMP12$^+$ cells in lung tissues of humans (right). (D) Representative immunoblots (left), and relative quantitative expressions (right) of MMP12, TIMP1, and elastin in lung tissues of humans. (E) Representative images (left) of F4/80 and CD206 immunostaining in lung tissues of mice (scale bars, 20 μm). The numbers (right) of F4/80$^+$CD206$^+$ cells in lung tissues of mice. (F) Representative immunoblots (left), and relative quantitative expressions (right) of ARG1 in lung tissues of mice. (G) Representative images (left) of CD206 and MMP12 immunostaining in lung tissues of mice (scale bars, 20 μm). The numbers of CD206$^+$MMP12$^+$ cells in lung tissues of mice (right). (H) Representative immunoblots (left), and relative quantitative expressions (right) of MMP12, TIMP1, and elastin in lung tissues of mice. Data represent means ± SEM. $^{**}P < 0.01$, compared with Non-smokers group or compared with 0 mg/m^3 TPM CS group.

located in CD68$^+$ macrophages (Fig. S6). Together, these findings show that, in CSE-treated macrophages, the expression of circADAMTS6 is abundant and stable.

3.3. *In CSE-treated macrophages, circADAMTS6 is involved in M2 polarization and in a proteinase/anti-proteinase imbalance*

To determine the influence of CS on macrophage polarization, we cultured murine BMDMs (Fig. S7A). For CSE-treated BMDMs, flow cytometry analysis revealed elevated numbers of F4/80$^+$CD206$^+$ M2 macrophages (Fig. S7B). Consistent with flow cytometry results, immunofluorescence and immunoblots demonstrated that CD206 and ARG1, markers for M2 macrophages, were elevated (Fig. S7C and S7D). Immunofluorescence experiments confirmed that levels of MMP12 in CD206$^+$ M2 macrophages were high (Fig. S7E). Further, levels of MMP12 protein and mRNA were elevated, but levels of TIMP1 protein and mRNA were lower (Fig. S7D and S7F). The levels of elastin degradation activity of CSE-treated BMDMs were high (Fig. S7G). Further, we found the same effects with CSE-treated THP-Ms (Fig. S8). These results reveal that elevated M2 polarization, and a proteinase/anti-proteinase imbalance in CSE-treated macrophages.

Next, to clarify the function of circADAMTS6 in M2 macrophage polarization, we down-regulated circADAMTS6 in CSE-treated THP-Ms (Fig. 4A). Flow cytometry analysis demonstrated that downregulation of circADAMTS6 decreased the CSE-induced elevated numbers of CD11b$^+$CD206$^+$ M2 macrophages and ARG1 protein levels, but not circAPBB1IP (Fig. 4B, 4C and Fig. S9). RNA-seq showed that expressions of TGM2 and ADORA3, M2-related genes, were significantly lower, as verified by qRT-PCR (Fig. S10A–C). For THP-Ms, downregulation of circADAMTS6 reversed the CSE-induced increased MMP12 protein and mRNA levels and decreased TIMP1 protein and mRNA levels (Fig. 4C, S10D and S10E). For CSE-treated THP-Ms, downregulation of circADAMTS6 blocked the increased levels of elastin degradation activity (Fig. 4D). We found the same results for CSE-treated RAW264.7 cells, a murine macrophage cell line (Fig. S11). These results indicate that, in CSE-treated macrophages, circADAMTS6 participates in M2 polarization and in a proteinase/anti-proteinase imbalance.

3.4. *circADAMTS6 activates CREB via CAMK2A in CSE-treated macrophages*

To elucidate the mechanism of circADAMTS6 in CS-induced M2 macrophage polarization, we performed RNA-seq for CSE-treated THP-Ms transfected with or without circADAMTS6 siRNA (Fig. 4E). Bioinformatic analysis revealed 751 differentially expressed genes ($P < 0.05$ and $|\log^2 FC| > 1.0$), of which 431 genes were down-regulated and

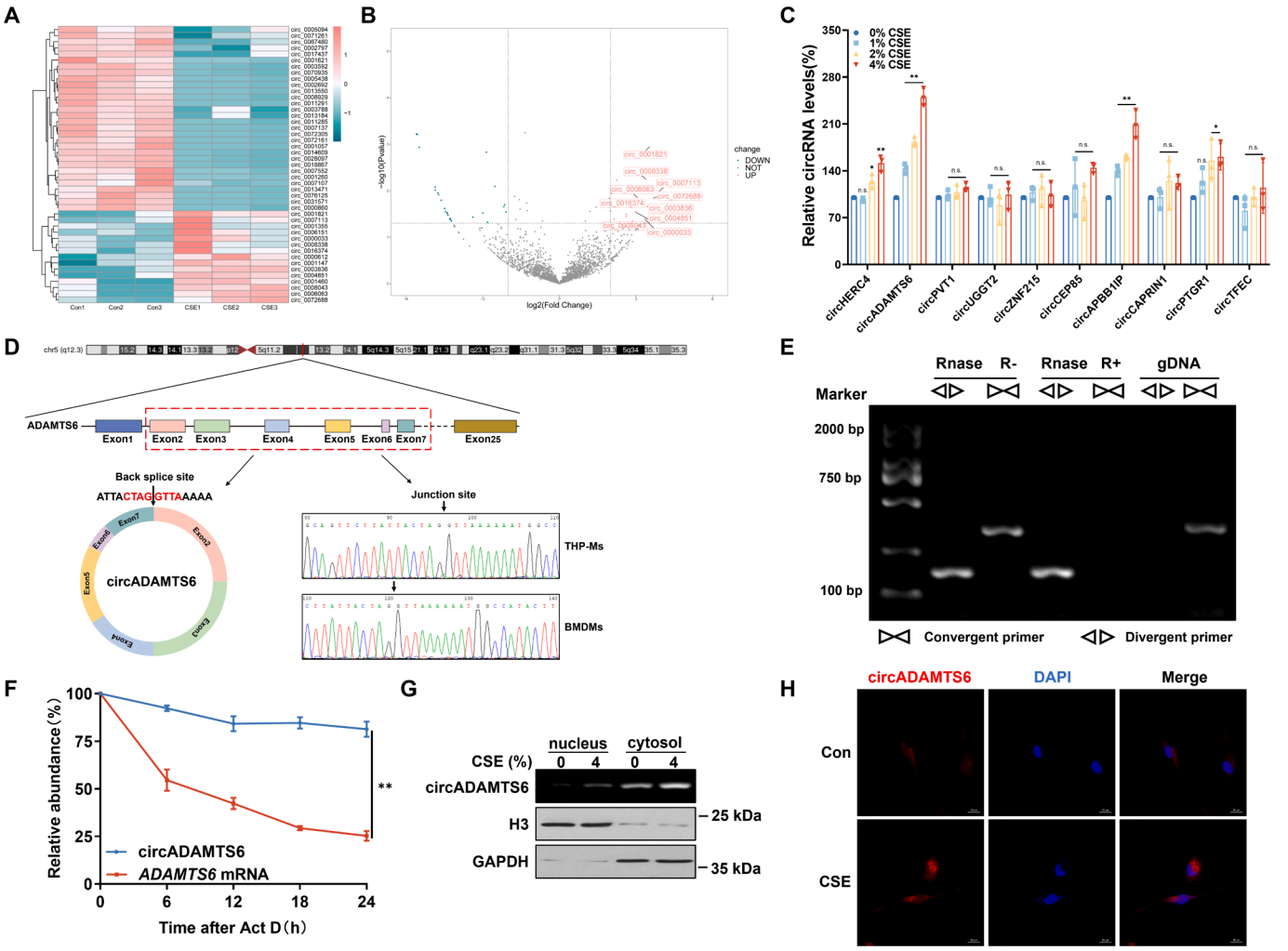

Fig. 3. Identification and characterization of circADAMTS6 in CSE-treated THP-Ms. THP-Ms were treated with 0 %, 1 %, 2 %, or 4 % CSE for 48 h. (A) Heatmap showing differentially expressed circRNAs in THP-Ms. (B) Volcano plot showing the top 10 up-regulated circRNAs in THP-Ms. (C) Levels of the top ten up-regulated circRNAs in THP-Ms as measured by qRT-PCR. (D) Schematic representation showing that circADAMTS6 was cyclized by six exons from the ADAMTS6 gene and Sanger sequencing for the back-splicing junction in THP-Ms (top) and BMDMs (bottom). (E) Agarose gel electrophoresis (AGE) showing the expression of circADAMTS6 and ADAMTS6 in THP-Ms treated with or without RNase R. (F) The abundances of circADAMTS6 and ADAMTS6 in THP-Ms were measured by qRT-PCR. (G) The expression of circADAMTS6 in the cytoplasm and nuclei of THP-Ms. (H) The localization of circADAMTS6 in THP-Ms was assessed by RNA fluorescence *in situ* hybridization (scale bars: 20 μm). Data represent means ± SD (n = 3). $^{*}P < 0.05$, $^{**}P < 0.01$, compared with 0 % CSE-treated cells or *ADAMTS6* mRNA. n.s., no significance.

320 genes were up-regulated, compared to CSE-treated THP-Ms (Fig. 4F and 4G). KEGG analysis showed that the cAMP signaling pathway was enriched (Fig. 4H). Prostaglandin E2 activates the cAMP-CREB signaling pathway to promote M2 macrophage polarization (Yang et al., 2019). During bone regeneration, adenosine promotes M2 macrophage polarization by activating the cAMP pathway through the A2b adenosine receptor (Sun et al., 2024). Our results demonstrated that, for macrophages, downregulation of circADAMTS6 inhibited the CSE-induced activation of CREB (Fig. 4I and S12). We assessed the upregulated and downregulated genes by KEGG pathway analysis and found that the cAMP signaling pathway was both upregulated and downregulated after downregulating circADAMTS6 (Fig. S13). Further, levels of CAMK2A, CAMK2B, NRP1, GLI, ATP1A2, and ATP1B2 were low and levels of AHM, HCAR2, ATP2B1, PDE4B, FOS and NFKBIA were high, compared to those of CSE-treated THP-Ms (Fig. S14A). These are mediators of the cAMP signaling pathway. We excluded HCAR3, which is not homologous for human and mice (Kapolka and Isom, 2020). Next, For CSE-treated macrophages, qRT-PCR verification showed that the mRNA levels of *CAMK2A*, *CAMK2B*, and *GLI1* were suppressed and the mRNA levels of *PDE4B* were recovered after downregulating circADAMTS6 (Fig. S14B and S14C). Further, RNA pull-down assays showed that circADAMTS6 interacted with CAMK2A (Fig. S14D). For CSE-treated macrophages, CAMK2A protein levels decreased with lower levels of circADAMTS6 (Figs. 4I and S12). In addition, in THP-Ms, downregulation of CAMK2A blocked CSE-induced activation of CREB (Fig. S15). These results show that, in CSE-treated macrophages, circADAMTS6 activates CREB via CAMK2A.

3.5. *A circADAMTS6/IGF2BP2/CAMK2A RNA-protein ternary complex stabilizes CAMK2A mRNA*

We used the RNA Interactome Database (Kang et al., 2022) to predict the interaction between circADAMTS6 and the *CAMK2A* mRNA 3′UTR (Fig. 5A), and RNA pull-down assays confirmed this interaction (Fig. 5B). Next, for CSE-treated THP-Ms, downregulation of circADAMTS6 inhibited elevation of luciferase mRNA and the luciferase activity of CAMK2A-WT (Fig. 5C). For THP-Ms, knockdown of circADAMTS6 reduced the half-life of *CAMK2A* (Fig. 5D). We also found that downregulation of circADAMTS6 in CSE-treated THP-Ms did not reduce CAMK2A protein degradation (Fig. S16). These results suggest

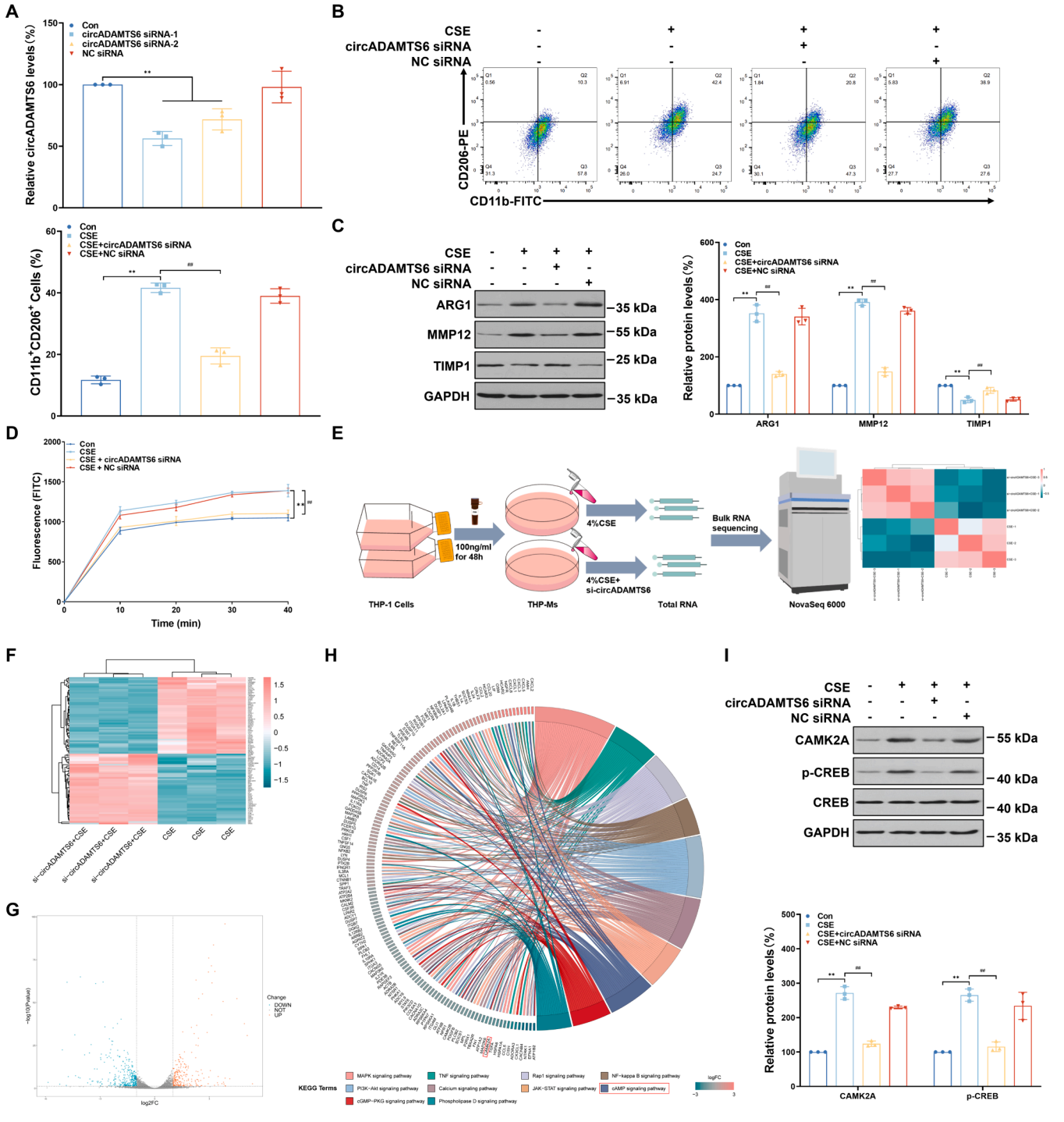

Fig. 4. circADAMTS6 is involved in M2 polarization, the proteinase/anti-proteinase imbalance, and activation of the cAMP signaling pathway in CSE-treated THP-Ms. THP-Ms were treated with 4 % CSE for 48 h after transfection with circADAMTS6 siRNA or NC siRNA for 6 h. (A) The levels of circADAMTS6 in THP-Ms were measured by qRT-PCR. (B) Representative flow cytometry plots (top) and quantification (bottom) of $CD11b^{+}CD206^{+}$ macrophages in THP-Ms. (C) Representative immunoblots (left), and relative quantitative expressions (right) of ARG1, MMP12, and TIMP1 in THP-Ms. (D) The levels of elastin degradation activity of THP-Ms were measured by fluorescence. (E) Schematic chart of workflow. Total RNA was extracted from THP-Ms treated with 4 % CSE for 48 h following transfection with circADAMTS6 siRNA or NC siRNA and then subjected to RNA sequencing. Heatmap (F) and Volcano plot (G) of differentially expressed genes in RNA sequencing. (H) Chord plot of KEGG functional enrichment analysis of the dysregulated genes. (I) Representative immunoblots (top) and relative quantitative expressions (bottom) of CAMK2A and p-CREB in THP-Ms. Data represent means ± SD (n = 3). $^{**}P < 0.01$, compared with 0 % CSE-treated cells. $^{\#\#}P < 0.01$, compared with 4 % CSE-treated cells.

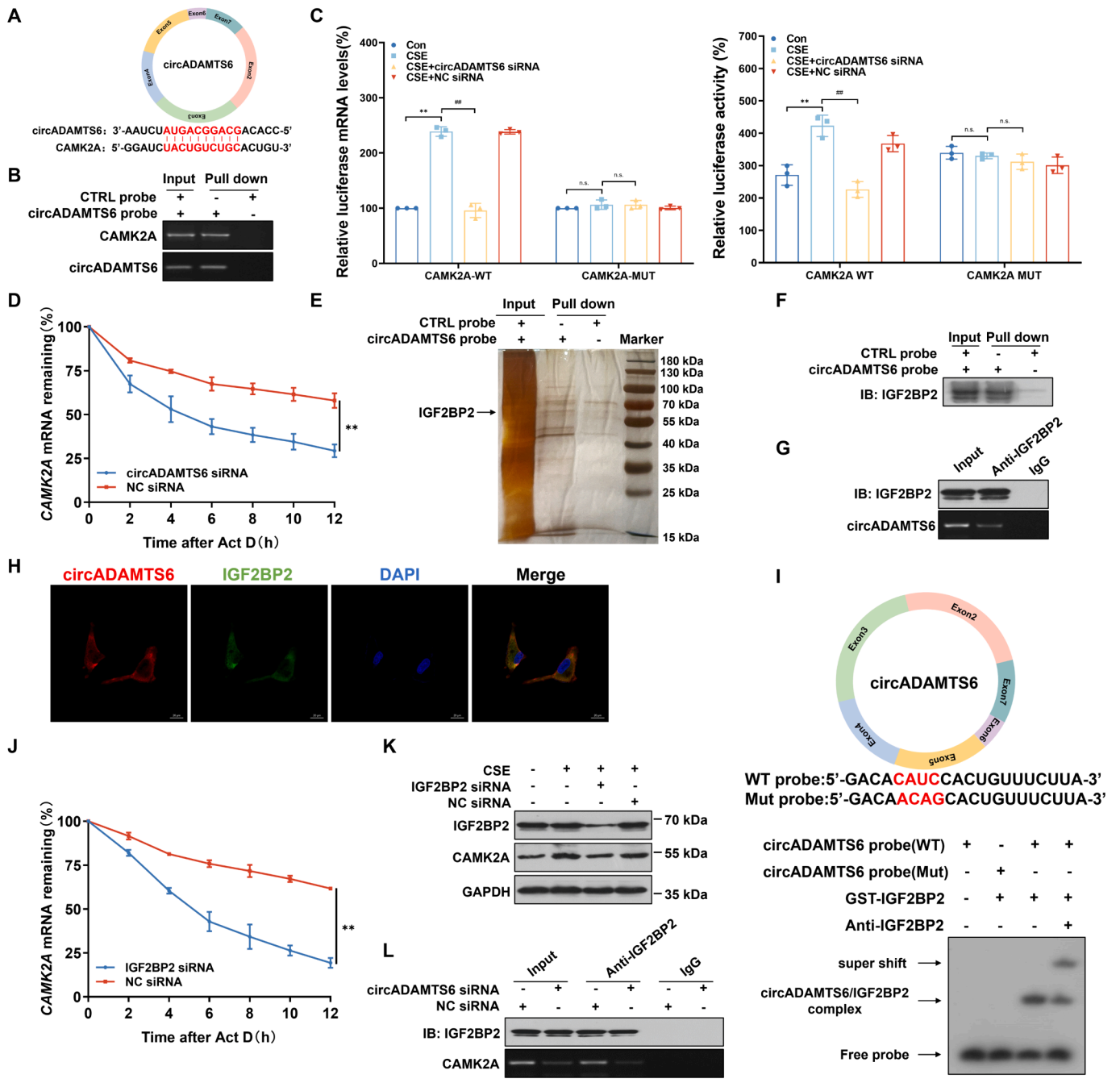

Fig. 5. Enhancement of circADAMTS6 increases CAMK2A levels through recruiting IGF2BP2 to stabilize CAMK2A mRNA in CSE-treated THP-Ms. THP-Ms were treated with 4 % CSE for 48 h. (A) RNA Sequence showing the binding site between circADAMTS6 and 3′UTR of CAMK2A. (B) AGE showed that circADAMTS6 was associated with CAMK2A, as determined by an RNA pull-down assay. (C) Relative luciferase mRNA levels (left) and luciferase activity (right) of a luciferase reporter gene containing either CAMK2A-WT or CAMK2A-MUT in CSE-treated THP-Ms transfected with circADAMTS6 siRNA or NC siRNA for 6 h. (D) The abundances of CAMK2A in THP-Ms transfected with circADAMTS6 siRNA or NC siRNA for 6 h were measured by qRT-PCR. (E) Identification of the potential proteins pulled down by a circADAMTS6 probe or circADAMTS6 anti-probe in THP-Ms. (F) Representative immunoblots of IGF2BP2 showing its interaction with circADAMTS6, as determined by an RNA pull-down assay. (G) The association of IGF2BP2 with circADAMTS6 as assessed by RIP assays of THP-Ms. (H) circADAMTS6 was co-localized with IGF2BP2 protein in the cytoplasm, as shown by RNA fluorescence *in situ* hybridization. (I) RNA-EMSA assays showing the binding capacity of purified IGF2BP2 with biotin-labeled oligonucleotides containing the CAUC motif from circADAMTS6. (J) The abundance of CAMK2A in THP-Ms transfected with IGF2BP2 siRNA or NC siRNA for 6 h were measured by qRT-PCR. (K) Representative immunoblots of IGF2BP2 and CAMK2A of CSE-treated THP-Ms transfected with IGF2BP2 siRNA or NC siRNA. (L) The association of IGF2BP2 with CAMK2A was determined by RIP assays of THP-Ms transfected with circADAMTS6 siRNA or NC siRNA. Data represent means ± SD (n = 3). $^{**}P < 0.01$, compared with 0 % CSE-treated, circADAMTS6 siRNA-treated, or IGF2BP2 siRNA-treated cells. $^{\#\#}P < 0.01$, compared with 4 % CSE-treated cells. n.s., no significant.

that circADAMTS6 regulates CAMK2A expression by affecting its mRNA stability.

circNSUN2, acting via IGF2BP2, an RNA-binding protein, enhances the stability of HMGA2 mRNA (Chen et al., 2019). By use of RNA pull-down assays followed by mass spectrometry analysis, we demonstrated that IGF2BP2 interacted with circADAMTS6 (Fig. 5E and 5F) (Table S2). RNA immunoprecipitation (RIP) assays confirmed that IGF2BP2 binds to circADAMTS6 (Fig. 5G). Immunofluorescence and

FISH assays showed that circADAMTS6 was expressed simultaneously in the cytoplasm with IGF2BP2 (Fig. 5H). catRAPID omics v2.0 (Armaos et al., 2021) was used to predict the propensity of the interaction between circADAMTS6 and IGF2BP2 (Fig. S17). The sequence CAUH (H = A, U, or C) is considered to be the only motif for recognizing IGF2BP2 (Hafner et al., 2010). By performing RNA-EMSA for THP-Ms, we confirmed that circADAMTS6 interacted with IGF2BP2 via the CAUC motif, and that, when the motif was ACAG, circADAMTS6 did not bind to IGF2BP2. Moreover, super-shift experiments showed that IGF2BP2 bound specifically to CAUC (Fig. 5I). These data demonstrate that, in the cytoplasm, circADAMTS6 interacts with IGF2BP2 via the CAUC motif.

We found that, for THP-Ms, knockdown of IGF2BP2 shortened the half-life of CAMK2A (Fig. 5J and S18) and that, after knocking down IGF2BP2, CAMK2A protein levels were lower in CSE-treated THP-Ms (Fig. 5K). In CSE-treated THP-Ms, the protein levels of IGF2BP2 did not change after knocking down circADAMTS6, but the protein levels of CAMK2A were lower (Fig. S19). Furthermore, in RIP assays, down-regulation of circADAMTS6 reduced the RNA-protein interaction between IGF2BP2 and CAMK2A (Fig. 5L). These results indicate that circADAMTS6 interacts with IGF2BP2 to enhance the stability of *CAMK2A* mRNA and increases CAMK2A levels via forming a circADAMTS6/IGF2BP2/CAMK2A RNA-protein ternary complex.

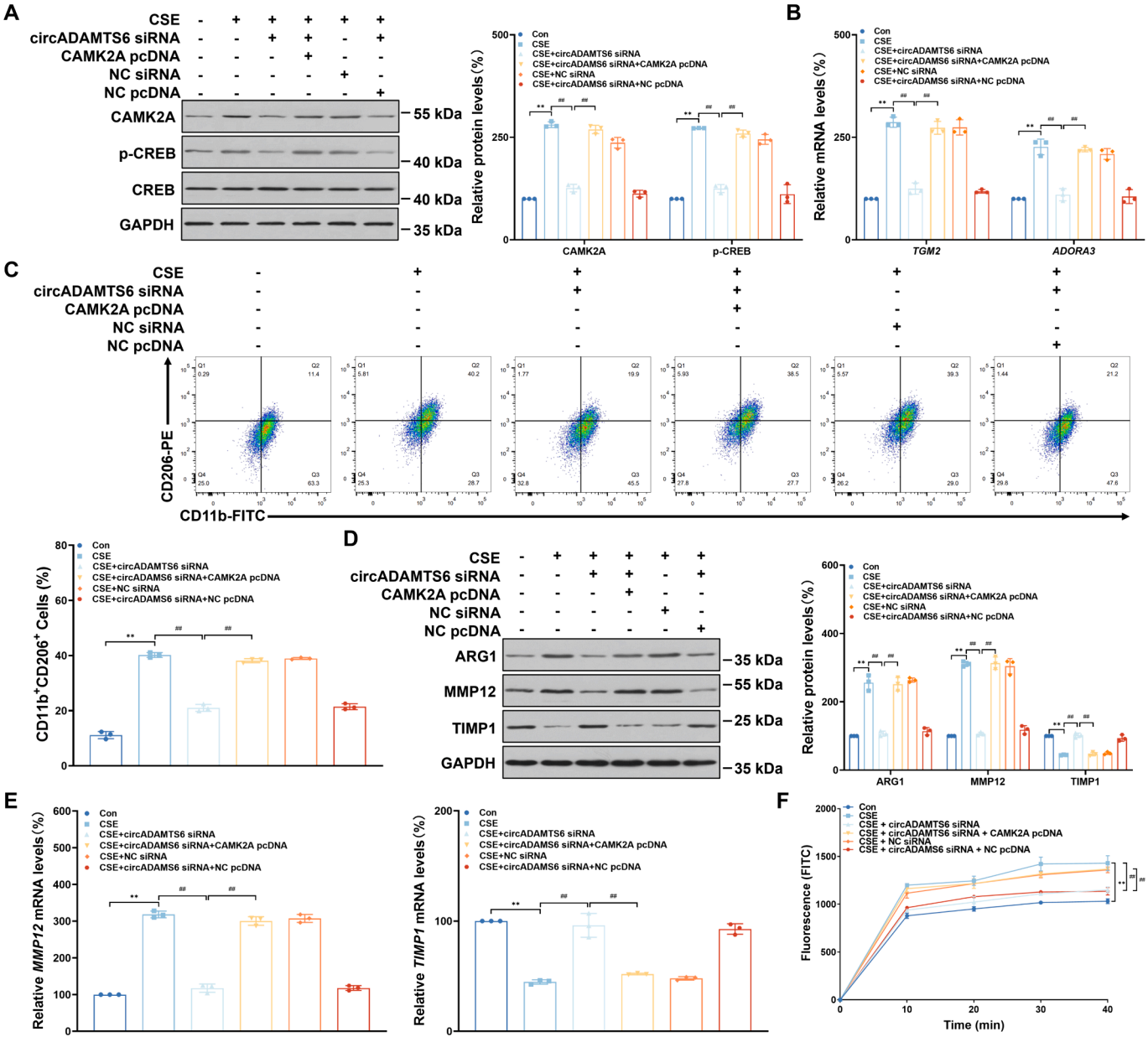

Fig. 6. circADAMTS6 activates CREB via CAMK2A to drive M2 polarization in CSE-treated THP-Ms. THP-Ms transfected with circADAMTS6 siRNA or CAMK2A pcDNA for 6 h were treated with 0 % or 4 % CSE for 48 h. (A) Representative immunoblots (left) and relative quantitative expressions (right) of CAMK2A and p-CREB in THP-Ms. (B) The levels of TGM2 and ADORA3 in THP-Ms were measured by qRT-PCR. (C) Representative flow cytometry plots (top) and quantification (bottom) of $CD11b^{+}CD206^{+}$ macrophages in THP-Ms. (D) Representative immunoblots (left) and relative quantitative expressions (right) of ARG1, MMP12, and TIMP1 in THP-Ms. (E) The levels of MMP12 and TIMP1 in THP-Ms were measured by qRT-PCR. (F) The levels of elastin degradation activity of THP-Ms were determined by fluorescence. Data represent means ± SD (n = 3). $^{**}P < 0.01$, compared with 0 % CSE-treated cells. $^{\#\#}P < 0.01$, compared with 4 % CSE-treated cells transfected with circADAMTS6 siRNA.

3.6. circADAMTS6 activates CREB via CAMK2A to drive M2 polarization in CSE-treated macrophages

To evaluate the effects of circADAMTS6-mediated activation of cAMP signaling and M2 polarization in macrophages, circADAMTS6 siRNA and CAMK2A pcDNA were transfected into CSE-treated macrophages. We used CAMK2A pcDNA to overexpress CAMK2A in THP-Ms (Fig. S20). For CSE-treated THP-Ms, knockdown of circADAMTS6 prevented the increase of CAMK2A and p-CREB. However, upregulation of CAMK2A reversed this effect (Fig. 6A). The CSE-induced levels of TGM2 and ADORA3 mRNA were reduced by knocking down circADAMTS6, but this influence was reversed after overexpression of CAMK2A (Fig. 6B). Flow cytometry analysis indicated that the CSE-induced increased numbers of $CD11b^{+}CD206^{+}$ M2 macrophages were lowered with the downregulation of circADAMTS6, but M2 macrophages were increased after overexpression of CAMK2A (Fig. 6C). In addition, after knocking down circADAMTS6, the protein level of ARG1 was lower in CSE-treated THP-Ms; this influence was reversed after upregulation of CAMK2A (Fig. 6D). Compared with the downregulation of circADAMTS6 alone, co-transfection of circADAMTS6 siRNA and CAMK2A pcDNA in CSE-treated THP-Ms reversed the decrease in MMP12 protein and mRNA levels and blocked the increase in TIMP1 protein and mRNA levels (Fig. 6D and 6E). Knockdown of circADAMTS6 reduced the elastin degradation activity of THP-Ms exposed to CSE, and overexpression of

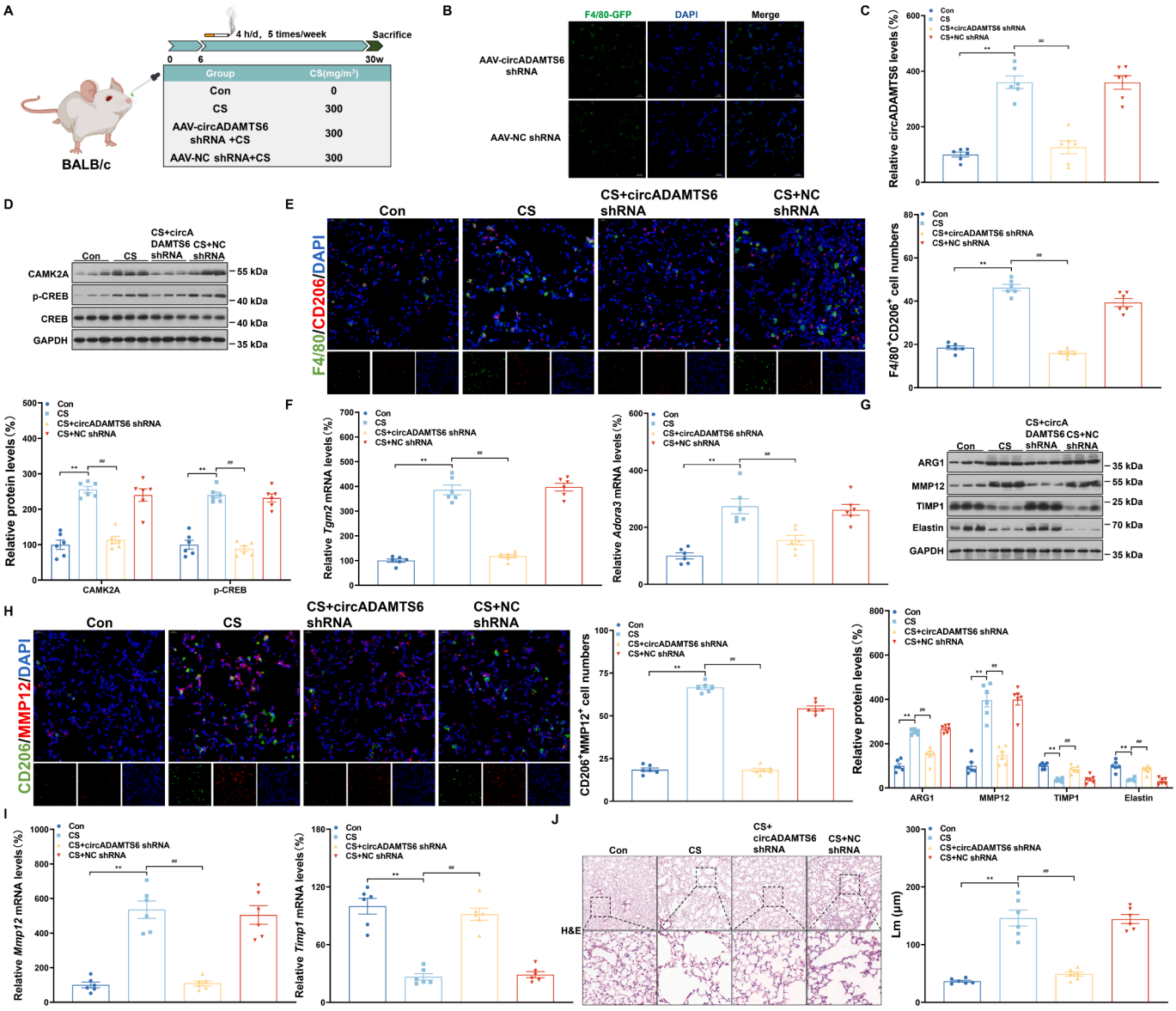

Fig. 7. Silencing of circADAMTS6 alleviates alveoli destruction through blocking M2 macrophage polarization in mice with CS-induced emphysema. (A) Schematic chart of workflow. Male BALB/c mice at 6 weeks of age treated with AAV-circADAMTS6 shRNA or AAV-NC shRNA were exposed to CS (0 or 300 mg/m^3 TPM) for 24 weeks. (B) Representative images of the AAV-circADAMTS6 shRNA and AAV-NC shRNA infection efficiencies in lung tissues of mice (scale bars, 20 μm). (C) In lung tissues of mice, the levels of circADAMTS6 were measured by qRT-PCR. (D) Representative immunoblots (top) and relative quantitative expressions (bottom) of CAMK2A and p-CREB in lung tissues of mice. (E) Representative images (left) of F4/80 and CD206 immunostaining in lung tissues of mice (scale bars, 20 μm). The numbers of $F4/80^{+}$ $CD206^{+}$ cells in lung tissues of mice (right). (F) The levels of Tgm2 and Adora3 in mouse lung tissues as determined by qRT-PCR. (G) Representative immunoblots (top) and relative quantitative expressions (bottom) of ARG1, MMP12, TIMP1, and elastin in lung tissues of mice. (H) Representative images (left) of CD206 and MMP12 immunostaining in mouse lung tissues (scale bars, 20 μm). The numbers of $CD206^{+}$ $MMP12^{+}$ cells in lung tissues of mice (right). (I) The levels of Mmp12 and Timp1 in lung tissues of mice as determined by qRT-PCR. (J) Representative H&E-stained (left) and quantification (right) of mean chord lengths (Lm) in lung tissues of mice (scale bars, 100 μm and 20 μm). Data represent means ± SEM (n = 6). $^{**}P < 0.05$, compared with the 0 mg/m^3 TPM CS group. $^{\#\#}P < 0.01$, compared with the 300 mg/m^3 TPM CS group.

CAMK2A increased the elastin degradation activity (Fig. 6F). Furthermore, there were similar results for RAW264.7 cells (Fig. S21). These results indicate that, in CSE-treated macrophages, circADAMTS6 activates CREB via CAMK2A to drive M2 polarization and promotes the proteinase/anti-proteinase imbalance and the increased elastin degradation.

3.7. Target of circADAMTS6 in macrophages prevents against mice with CS-induced emphysema via M2 polarization

To investigate the influence of circADAMTS6 in mice with CS-induced emphysema, we used AAV-circADAMTS6 shRNA to target macrophages in mouse lung tissues (Fig. 7A). The efficacy of AAV-circADAMTS6 shRNA was examined by body weights, immunofluorescence staining, and qRT-PCR (Fig. S22 and 7B–C). Consistent with the in vitro experiments, the protein levels of CAMK2A and p-CREB were lowered in mouse lung tissues by silencing circADAMTS6 (Fig. 7D). Immunofluorescence staining showed that, in mouse lung macrophages, silencing of circADAMTS6 blocked the increased numbers of F4/80^{+}CD206^{+} M2 macrophages induced by CS (Fig. 7E). Tgm2 and Adora3 mRNA levels and the ARG1 protein levels were low (Fig. 7F and 7G). The numbers of MMP12^{+} cells in CD206^{+} M2 macrophages were decreased (Fig. 7H). Silencing of circADAMTS6 blocked the CS-induced proteinase/anti-proteinase imbalance, which was manifested primarily by blocking the higher protein and mRNA levels of MMP12 and restoring the lower protein and mRNA levels of TIMP1 induced by CS (Fig. 7G and 7I). Silencing of circADAMTS6 blocked the elastin degradation caused by CS (Fig. 7G) and the destruction of alveolar walls and enhancement of mean chord lengths (Fig. 7J). We found that Penh values were elevated in mice with CS-induced emphysema and were lower after downregulation of circADAMTS6 (Fig. S23). These results demonstrate that, in mice, targeting of circADAMTS6 inhibits the M2 macrophage polarization and protects CS-induced emphysema.

3.8. circADAMTS6 serves as a potential clinical marker for smoking-related emphysema

Organoids are practical for basic and clinical research, and have potential applications in disease modeling and treatment screening (Tang et al., 2022b). We constructed a co-culture model of macrophages and mice lung organoids following a published method (Wang et al., 2023) (Fig. 8A). We established the lung organ morphology by fluorescence microscopy, and characterized the surfactant protein-C-positive (SPC^{+}) alveolar organoids by immunofluorescence staining (Fig. 8B). The growth of organoids co-cultured with CSE-treated RAW264.7 cells was inhibited; this inhibition of growth was reversed by downregulation of circADAMTS6 (Fig. 8C and 8D). In addition, the expressions of SPC^{+} cells were low in organoids co-cultured with CSE-treated RAW264.7 cells, an effect that was reversed by downregulation of circADAMTS6 (Fig. S24). We also collected human serum (Table 1) and the serum levels of circADAMTS6 were elevated in Smokers and COPD smokers (Fig. 8E). They negatively correlated with FEV1/FVC (%) and with predicted FEV1 (%) as determined by Pearson correlation analysis (Fig. 8F). These results demonstrate that circADAMTS6 serves as a potential biomarker for smoking-related emphysema.

4. Discussion

Cigarette smoking is a serious public health problem, with approximately 20 % of the global population smoking; about half of them die from smoking-related disease (Rigotti et al., 2022). CS is a powerful driver of the development of COPD, and studies conducted on cohorts of individuals with COPD have demonstrated that, compared to low CS exposure, high CS exposure exacerbates the decline in lung function (Kim et al., 2021b). Emphysema, a primary form of COPD, is manifested as the destruction of airway walls leading to the pathological expansion of alveolar space caused by CS (Fu et al., 2022). Macrophages, as innate immune cells in the pulmonary system, have the capacity to recognize and process various environmental stimuli, including CS and particulate matter (Akata and van Eeden, 2020). In the lungs of COPD patients, CS affects the function and phenotype of macrophages (Kotlyarov, 2023). In the lungs of COPD patients, macrophages of both the M1 and M2 phenotypes are present and are associated with the severity of the disease (Lee et al., 2021). Here, the results of scRNAseq showed that the ratio of M2 macrophages was increased in the lungs of COPD patients and mice with CS-induced emphysema. M2 macrophages were elevated in lung tissues of Smokers and COPD smokers and in the lung tissues of mice with CS-induced emphysema.

The activation of macrophages is involved in regulating the degradation of elastin, a component of the ECM, and contributes to the pathogenesis of emphysema (Gharib et al., 2018). In addition, macrophages in emphysema induced by chronic CS exposure are biased toward the M2 phenotype, which, in a chronic inflammatory environment, promotes degradation of the ECM and leads to abnormal tissue repair (Gharib et al., 2018). However, how the degradation of ECM promoted by M2 macrophages is involved in CS-induced emphysema remains unclear. In bronchial asthma, respiratory syncytial virus-induced M2 polarization of macrophages produces MMP12, which leads to airway inflammation (Makino et al., 2021). By degrading elastin, MMP12 causes destruction of the alveolar structure, leading to emphysema (Lugg et al., 2022). Here, we found, increased MMP12 secreted by M2 macrophages. Decreased TIMP1 and elastin degradation were evident for Smokers and COPD smokers, and for mice with CS-induced emphysema. In addition, for CSE-treated macrophages, there were an increase in MMP12 expression, a decrease in TIMP1 expression, and an increase in elastin degradation. Therefore, these results show that, a proteinase/anti-proteinase imbalance and elastin degradation induced by M2 macrophage polarization are involved in the occurrence and development of smoking-related emphysema.

With the development of bioinformatics and high-throughput sequencing, circRNAs are now established as being widely present in various species and organs (Chen et al., 2021). They are involved in numerous cellular processes and are associated with the pathogenesis of various diseases (He et al., 2021). For mouse lung tissues, CS exposure causes dysregulated expression of circRNAs, which are involved in the progression of COPD (Chen et al., 2020). circRNAs have various functions in the regulation of differentiation and adaptation of macrophages and T cells (Zhang et al., 2020). In our research, circADAMTS6 was elevated and located in CSE-treated macrophages. For these macrophages, knockdown of circADAMTS6 inhibited the M2 polarization, which blocked the imbalance of proteinase/anti-proteinase and the elevation of elastin degradation activity. Consistent with the results for cultured cells, silencing of circADAMTS6 in macrophages of mice with CS-induced emphysema inhibited M2 polarization, which blocked the progression of CS-induced emphysema. Thus, we conclude that circADAMTS6 affects the progression of CS-induced emphysema by modulating the M2 polarization of macrophages.

In the cytoplasm, circRNAs regulate gene expression by forming functional circRNP complexes, acting as sponges for miRNAs, interacting with mRNAs, and/or interacting with proteins (Liu and Chen, 2022). IGF2BP1-3, a family of highly conserved proteins, regulate the stability, transport, and translation of mRNA through the use of a distinctive co-recognized sequence, CAUH (H = A, U, or C), functioning as RNA-binding proteins (Hafner et al., 2010). By stabilizing FGF9 mRNA through IGF2BP2, circITGB6 promotes the occurrence and development of ovarian cancers (Li et al., 2022). Herein, we demonstrate that circADAMTS6 interacts with IGF2BP2 to form a circADAMTS6/IGF2BP2/CAMK2A RNA-protein ternary complex that enhances stability of CAMK2A mRNA.

In the present study, we elucidated a mechanism by which circADAMTS6 regulates CS-induced M2 polarization in macrophages. We

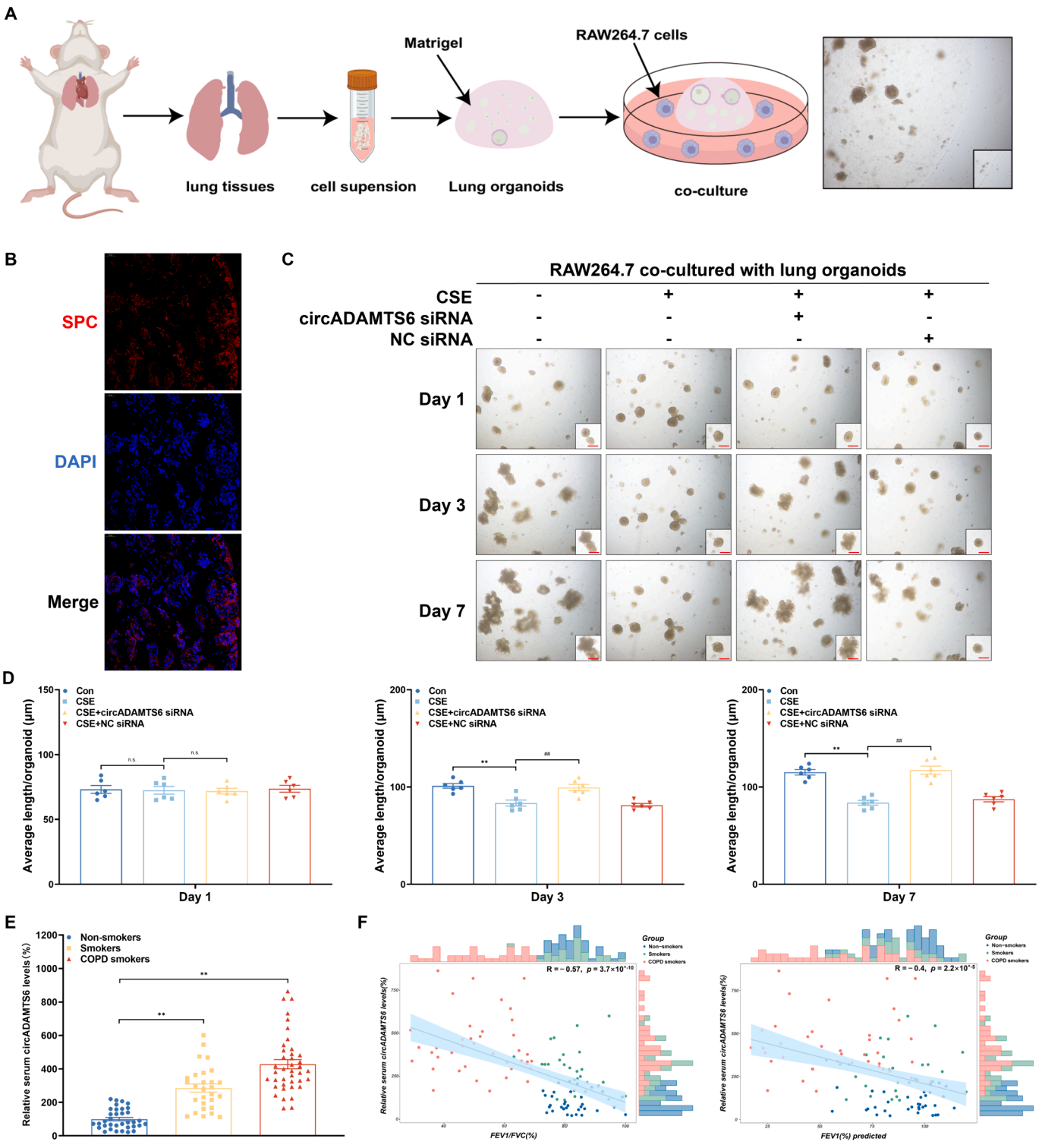

Fig. 8. Circadamts6 serves as a potential clinical marker for smoking-related emphysema. Human serum was collected from Non-smokers (n = 35), Smokers (n = 28), or COPD smokers (n = 40). RAW264.7 cells transfected with circADAMTS6 siRNA or NC siRNA for 6 h were treated with 4 % CSE for 48 h. (A) Schematic chart of workflow. Establishment of mouse lung organoids, they were co-cultured with RAW264.7 cells. (B) Representative images of SPC immunostaining in mouse lung organoids (scale bars, 50 μm). (C) Representative images of mouse lung organoids in light microscopy (scale bars, 100 μm). (D) The average diameters of mouse lung organoids. (E) The levels of circADAMTS6 in human serum were measured by qRT-PCR. (F) Pearson correlation analysis of serum circADAMTS6 with FEV1/FVC (%) or predicted FEV1 (%). Data represent means ± SEM. $^{**}P < 0.01$, compared with mouse lung organoids co-cultured with 0 % CSE-treated RAW264.7 cells or the Non-smokers group. $^{\#\#}P < 0.01$, compared with mouse lung organoids co-cultured with 4 % CSE-treated RAW264.7 cells.

performed RNA-seq in CSE-treated THP-Ms with knockdown of circADAMTS6 and found an enriched cAMP signaling pathway. This pathway acts as a cofactor in macrophage reprogramming and participates in M2 macrophage polarization through the phosphorylation of CREB (Zhao et al., 2022). After knockdown of circADAMTS6, CAMK2A causes obvious changes in the cAMP signaling pathway; it may have a regulatory relationship. In microglia, CAMK2A activates phosphorylation of CREB to maintain synaptic plasticity (More et al., 2022). Moreover, phosphorylated CREB contributes to M2 polarization of macrophages (Jiang et al., 2022; Luan et al., 2015). Our results confirm that circADAMTS6 promotes the activation of CREB via CAMK2A to promote M2 polarization in CSE-treated macrophages.

Lung organoids are used to simulate lung diseases and to provide new therapeutic targets for these diseases (Liberti and Morrisey, 2021). Compared to two-dimensional disease models, the three-dimensional organoid model better reflects the interaction between cells and the ECM (Kim et al., 2021a). Therefore, to evaluate the role of M2 macrophages in emphysema, we established a co-culture model of macrophages and lung organoids. After knockdown of circADAMTS6 in CSE-treated RAW264.7 cells, the growth of organoids was restored. We also note that circRNAs are potential targets for disease diagnosis and treatment (Chen et al., 2022). In our research, we found that, in the serum of Smokers and COPD smokers, the levels of circADAMTS6 were elevated and negatively correlated with lung function. Thus, circADAMTS6 may serve as a clinical biomarker for smoking-related emphysema.

In summary, we provide a newly identified mechanism for circADAMTS6 in CS-induced emphysema. This factor regulates M2 polarization, proteinase/anti-proteinase imbalance, and elastin degradation in CSE-treated macrophages and in a mouse model of CS-induced emphysema. Further, M2 macrophage polarization is involved in the pathogenesis of smoking-related COPD. In addition, elevated circADAMTS6 levels in smoking-related COPD are inversely correlated with lung function, providing a potential marker for COPD diagnosis.

5. Conclusion

Our results demonstrate that polarization of circADAMTS6-driven M2 macrophages has an essential function in CS-induced emphysema. With CS exposure, elevated circADAMTS6 interacts with IGF2BP2 to form a circADAMTS6/IGF2BP2/CAMK2A RNA-protein ternary complex that enhances the stability of CAMK2A mRNA. Subsequently, elevated CAMK2A activates CREB to promote the M2 polarization of macrophages, leading to a proteinase/anti-proteinase imbalance and elastin degradation that triggers emphysema. In addition, in the serum of smokers and COPD smokers, the levels of circADAMTS6 are elevated and negatively correlate with lung function. Therefore, circADAMTS6-driven M2 polarization in macrophages may serve as a diagnostic and/or therapeutic marker for CS-induced emphysema.

CRediT authorship contribution statement

Jiaheng Lin: Writing – original draft, Visualization, Validation, Methodology, Investigation, Funding acquisition, Formal analysis. **Haibo Xia:** Writing – review & editing, Methodology, Conceptualization. **Jinyan Yu:** Validation, Methodology, Investigation, Formal analysis. **Yue Wang:** Validation, Methodology, Investigation, Formal analysis. **Hailan Wang:** Validation, Methodology. **Daxiao Xie:** . **Cheng Cheng:** Validation, Investigation. **Lu Lu:** Funding acquisition. **Tao Bian:** Writing – review & editing, Methodology, Conceptualization. **Yan Wu:** Supervision, Methodology, Funding acquisition, Conceptualization. **Qizhan Liu:** Writing – review & editing, Supervision, Resources, Project administration, Funding acquisition, Conceptualization.

Declaration of competing interest

The authors declare that they have no known competing financial interests or personal relationships that could have appeared to influence the work reported in this paper.

Data availability

The data that support the findings of this study are available from the corresponding authors on reasonable request.

Acknowledgements and funding

The authors thank Donald L. Hill (University of Alabama at Birmingham, USA), an experienced, English-speaking scientific editor, for editing. This work was supported by the Natural Science Foundations of China (82173472, 82173563, 81973085); and Major Program of Wuxi Medical Center, Nanjing Medical University (WMCM202309); and the Priority Academic Program Development of Jiangsu Higher Education Institutions (2023); and 2022 Jiangsu Postgraduate Scientific Research Innovation Plan (SJCX22_0674).

Appendix A. Supplementary material

Supplementary data to this article can be found online at https://doi.org/10.1016/j.envint.2024.108832.

References

Akata, K., van Eeden, S.F., 2020. Lung macrophage functional properties in chronic obstructive pulmonary disease. Int. J. Mol. Sci. 21.
Armaos, A., Colantoni, A., Proietti, G., Rupert, J., Tartaglia, G.G., 2021. catRAPID omics v2.0: going deeper and wider in the prediction of protein-RNA interactions. Nucleic Acids Res. 49, W72–W79.
Belchamber, K.B.R., Donnelly, L.E., 2020. Targeting defective pulmonary innate immunity - a new therapeutic option? Pharmacol. Ther. 209, 107500.
Bracke, K.R., Verhamme, F.M., Seys, L.J., Bantsimba-Malanda, C., Cunoosamy, D.M., Herbst, R., Hammad, H., Lambrecht, B.N., Joos, G.F., Brusselle, G.G., 2013. Role of CXCL13 in cigarette smoke-induced lymphoid follicle formation and chronic obstructive pulmonary disease. Am. J. Respir. Crit. Care Med. 188, 343–355.
Chen, R.X., Chen, X., Xia, L.P., Zhang, J.X., Pan, Z.Z., Ma, X.D., Han, K., Chen, J.W., Judde, J.G., Deas, O., Wang, F., Ma, N.F., Guan, X., Yun, J.P., Wang, F.W., Xu, R.H., Dan, X., 2019. N(6)-methyladenosine modification of circNSUN2 facilitates cytoplasmic export and stabilizes HMGA2 to promote colorectal liver metastasis. Nat. Commun. 10, 4695.
Chen, L., Wang, C., Sun, H., Wang, J., Liang, Y., Wang, Y., Wong, G., 2021. The bioinformatics toolbox for circRNA discovery and analysis. Brief. Bioinform. 22, 1706–1728.
Chen, Y., Wang, J., Wang, C., Liu, M., Zou, Q., 2022. Deep learning models for disease-associated circRNA prediction: a review. Brief. Bioinform. 23.
Chen, S., Yao, Y., Lu, S., Chen, J., Yang, G., Tu, L., Chen, L., 2020. CircRNA0001859, a new diagnostic and prognostic biomarkers for COPD and AECOPD. BMC Pulm. Med. 20, 311.
Cheng, C., Wang, P., Yang, Y., Du, X., Xia, H., Liu, J., Lu, L., Wu, H., Liu, Q., 2023. Smoking-induced M2-TAMs, via circEML4 in EVs, promote the progression of NSCLC through ALKBH5-regulated m6A modification of SOCS2 in NSCLC cells. Adv. Sci. (Weinh.) 10, e2300953.
Christenson, S.A., Smith, B.M., Bafadhel, M., Putcha, N., 2022. Chronic obstructive pulmonary disease. Lancet 399, 2227–2242.
Collaborators, G.B.D.T., 2021. Spatial, temporal, and demographic patterns in prevalence of smoking tobacco use and attributable disease burden in 204 countries and territories, 1990–2019: a systematic analysis from the Global Burden of Disease Study 2019. Lancet 397, 2337–2360.
Dong, T., Chen, X., Xu, H., Song, Y., Wang, H., Gao, Y., Wang, J., Du, R., Lou, H., Dong, T., 2022. Mitochondrial metabolism mediated macrophage polarization in chronic lung diseases. Pharmacol. Ther. 239, 108208.
Doyle, A.D., Mukherjee, M., LeSuer, W.E., Bittner, T.B., Pasha, S.M., Frere, J.J., Neely, J. L., Kloeber, J.A., Shim, K.P., Ochkur, S.I., Ho, T., Svenningsen, S., Wright, B.L., Rank, M.A., Lee, J.J., Nair, P., Jacobsen, E.A., 2019. Eosinophil-derived IL-13 promotes emphysema. Eur. Respir. J. 53.
Eapen, M.S., Hansbro, P.M., McAlinden, K., Kim, R.Y., Ward, C., Hackett, T.L., Walters, E. H., Sohal, S.S., 2017. Abnormal M1/M2 macrophage phenotype profiles in the small airway wall and lumen in smokers and chronic obstructive pulmonary disease (COPD). Sci. Rep. 7, 13392.
Fu, Y.S., Kang, N., Yu, Y., Mi, Y., Guo, J., Wu, J., Weng, C.F., 2022. Polyphenols, flavonoids and inflammasomes: the role of cigarette smoke in COPD. Eur. Respir. Rev. 31.

Fu, X., Shi, H., Qi, Y., Zhang, W., Dong, P., 2015. M2 polarized macrophages induced by CSE promote proliferation, migration, and invasion of alveolar basal epithelial cells. Int. Immunopharmacol. 28, 666–674.
Gharib, S.A., Manicone, A.M., Parks, W.C., 2018. Matrix metalloproteinases in emphysema. Matrix Biol. 73, 34–51.
Gould, T.J., 2023. Epigenetic and long-term effects of nicotine on biology, behavior, and health. Pharmacol. Res. 192, 106741.
Hafner, M., Landthaler, M., Burger, L., Khorshid, M., Hausser, J., Berninger, P., Rothballer, A., Ascano Jr., M., Jungkamp, A.C., Munschauer, M., Ulrich, A., Wardle, G.S., Dewell, S., Zavolan, M., Tuschl, T., 2010. Transcriptome-wide identification of RNA-binding protein and microRNA target sites by PAR-CLIP. Cell 141, 129–141.
Hartog, M., Zhang, Q.Y., Ding, X., 2019. Role of mouse cytochrome P450 enzymes of the Cyp2abfgs subfamilies in the induction of lung inflammation by cigarette smoke exposure. Toxicol. Sci. 172, 123–131.
Hautamaki, R.D., Kobayashi, D.K., Senior, R.M., Shapiro, S.D., 1997. Requirement for macrophage elastase for cigarette smoke-induced emphysema in mice. Science 277, 2002–2004.
He, A.T., Liu, J., Li, F., Yang, B.B., 2021. Signal Transduct. Target. Ther. 6, 185.
He, S., Xie, L., Lu, J., Sun, S., 2017. Characteristics and potential role of M2 macrophages in COPD. Int. J. Chron. Obstruct. Pulmon. Dis. 12, 3029–3039.
Hisata, S., Racanelli, A.C., Kermani, P., Schreiner, R., Houghton, S., Palikuqi, B., Kunar, B., Zhou, A., McConn, K., Capili, A., Redmond, D., Nolan, D.J., Ginsberg, M., Ding, B.S., Martinez, F.J., Scandura, J.M., Cloonan, S.M., Rafii, S., Choi, A.M.K., 2021. Reversal of emphysema by restoration of pulmonary endothelial cells. J. Exp. Med. 218.
Ishii, T., Abboud, R.T., Wallace, A.M., English, J.C., Coxson, H.O., Finley, R.J., Shumansky, K., Pare, P.D., Sandford, A.J., 2014. Alveolar macrophage proteinase/antiproteinase expression in lung function and emphysema. Eur. Respir. J. 43, 82–91.
Jang, E.S., Jeong, S.H., Hwang, S.H., Kim, H.Y., Ahn, S.Y., Lee, J., Lee, S.H., Park, Y.S., Hwang, J.H., Kim, J.W., Kim, N., Lee, D.H., 2012. Effects of coffee, smoking, and alcohol on liver function tests: a comprehensive cross-sectional study. BMC Gastroenterol. 12, 145.
Jiang, H., Wei, H., Wang, H., Wang, Z., Li, J., Ou, Y., Xiao, X., Wang, W., Chang, A., Sun, W., Zhao, L., Yang, S., 2022. Zeb1-induced metabolic reprogramming of glycolysis is essential for macrophage polarization in breast cancer. Cell Death Dis. 13, 206.
Kang, J., Tang, Q., He, J., Li, L., Yang, N., Yu, S., Wang, M., Zhang, Y., Lin, J., Cui, T., Hu, Y., Tan, P., Cheng, J., Zheng, H., Wang, D., Su, X., Chen, W., Huang, Y., 2022. RNAInter v4.0: RNA interactome repository with redefined confidence scoring system and improved accessibility. Nucleic Acids Res. 50, D326–D332.
Kapolka, N.J., Isom, D.G., 2020. HCAR3: an underexplored metabolite sensor. Nat. Rev. Drug Discov. 19, 745.
Kim, S.K., Kim, Y.H., Park, S., Cho, S.W., 2021a. Organoid engineering with microfluidics and biomaterials for liver, lung disease, and cancer modeling. Acta Biomater. 132, 37–51.
Kim, W., Moll, M., Qiao, D., Hobbs, B.D., Shrine, N., Sakornsakolpat, P., Tobin, M.D., Dudbridge, F., Wain, L.V., Ladd-Acosta, C., Chatterjee, N., Silverman, E.K., Cho, M. H., Beaty, T.H., 2021b. Interaction of cigarette smoking and polygenic risk score on reduced lung function. JAMA Netw. Open 4, e2139525.
Kotlyarov, S., 2023. The role of smoking in the mechanisms of development of chronic obstructive pulmonary disease and atherosclerosis. Int. J. Mol. Sci. 24.
Kulikauskaite, J., Wack, A., 2020. Teaching old dogs new tricks? The plasticity of lung alveolar macrophage subsets. Trends Immunol. 41, 864–877.
Kumar, D., Sahoo, S.S., Chauss, D., Kazemian, M., Afzali, B., 2023. Non-coding RNAs in immunoregulation and autoimmunity: technological advances and critical limitations. J. Autoimmun. 134, 102982.
Lee, J.W., Chun, W., Lee, H.J., Min, J.H., Kim, S.M., Seo, J.Y., Ahn, K.S., Oh, S.R., 2021. The role of macrophages in the development of acute and chronic inflammatory lung diseases. Cells 10.
Li, D., Li, Z., Yang, Y., Zeng, X., Li, Y., Du, X., Zhu, X., 2020. Circular RNAs as biomarkers and therapeutic targets in environmental chemical exposure-related diseases. Environ. Res. 180, 108825.
Li, H., Luo, F., Jiang, X., Zhang, W., Xiang, T., Pan, Q., Cai, L., Zhao, J., Weng, D., Li, Y., Dai, Y., Sun, F., Yang, C., Huang, Y., Yang, J., Tang, Y., Han, Y., He, M., Zhang, Y., Song, L., Xia, J.C., 2022. CircITGB6 promotes ovarian cancer cisplatin resistance by resetting tumor-associated macrophage polarization toward the M2 phenotype. J. Immunother. Cancer 10.
Liberti, D.C., Morrisey, E.E., 2021. Organoid models: assessing lung cell fate decisions and disease responses. Trends Mol. Med. 27, 1159–1174.
Liu, C.X., Chen, L.L., 2022. Circular RNAs: characterization, cellular roles, and applications. Cell 185, 2016–2034.
Liu, Z., Wang, T., She, Y., Wu, K., Gu, S., Li, L., Dong, C., Chen, C., Zhou, Y., 2021. N(6)-methyladenosine-modified circIGF2BP3 inhibits CD8(+) T-cell responses to facilitate tumor immune evasion by promoting the deubiquitination of PD-L1 in non-small cell lung cancer. Mol. Cancer 20, 105.
Luan, B., Yoon, Y.S., Le Lay, J., Kaestner, K.H., Hedrick, S., Montminy, M., 2015. CREB pathway links PGE2 signaling with macrophage polarization. PNAS 112, 15642–15647.
Lugg, S.T., Scott, A., Parekh, D., Naidu, B., Thickett, D.R., 2022. Cigarette smoke exposure and alveolar macrophages: mechanisms for lung disease. Thorax 77, 94–101.
Ma, Y., Long, Y., Chen, Y., 2021. Roles of inflammasome in cigarette smoke-related diseases and physiopathological disorders: mechanisms and therapeutic opportunities. Front. Immunol. 12, 720049.
Ma, Q., Yang, F., Huang, B., Pan, X., Li, W., Yu, T., Wang, X., Ran, L., Qian, K., Li, H., Li, H., Liu, Y., Liang, C., Ren, J., Zhang, Y., Wang, S., Xiao, B., 2022. CircARID1A binds to IGF2BP3 in gastric cancer and promotes cancer proliferation by forming a circARID1A-IGF2BP3-SLC7A5 RNA-protein ternary complex. J. Exp. Clin. Cancer Res. 41, 251.
Makino, A., Shibata, T., Nagayasu, M., Hosoya, I., Nishimura, T., Nakano, C., Nagata, K., Ito, T., Takahashi, Y., Nakamura, S., 2021. RSV infection-elicited high MMP-12-producing macrophages exacerbate allergic airway inflammation with neutrophil infiltration. iScience 24, 103201.
Misir, S., Wu, N., Yang, B.B., 2022. Specific expression and functions of circular RNAs. Cell Death Differ. 29, 481–491.
More, L., Privitera, L., Perrett, P., Cooper, D.D., Bonnello, M.V.G., Arthur, J.S.C., Frenguelli, B.G., 2022. CREB serine 133 is necessary for spatial cognitive flexibility and long-term potentiation. Neuropharmacology 219, 109237.
Pasupneti, S., Tian, W., Tu, A.B., Dahms, P., Granucci, E., Gandjeva, A., Xiang, M., Butcher, E.C., Semenza, G.L., Tuder, R.M., Jiang, X., Nicolls, M.R., 2020. Endothelial HIF-2alpha as a key endogenous mediator preventing emphysema. Am. J. Respir. Crit. Care Med. 202, 983–995.
Phillips, J.E., 2017. Inhaled efficacious dose translation from rodent to human: a retrospective analysis of clinical standards for respiratory diseases. Pharmacol. Ther. 178, 141–147.
Rigotti, N.A., Kruse, G.R., Livingstone-Banks, J., Hartmann-Boyce, J., 2022. Treatment of tobacco smoking: a review. J. Am. Med. Assoc. 327, 566–577.
Shaykhiev, R., Krause, A., Salit, J., Strulovici-Barel, Y., Harvey, B.G., O'Connor, T.P., Crystal, R.G., 2009. Smoking-dependent reprogramming of alveolar macrophage polarization: implication for pathogenesis of chronic obstructive pulmonary disease. J. Immunol. 183, 2867–2883.
Soleimani, F., Dobaradaran, S., De-la-Torre, G.E., Schmidt, T.C., Saeedi, R., 2022. Content of toxic components of cigarette, cigarette smoke vs cigarette butts: a comprehensive systematic review. Sci. Total Environ. 813, 152667.
Spix, B., Butz, E.S., Chen, C.C., Rosato, A.S., Tang, R., Jeridi, A., Kudrina, V., Plesch, E., Wartenberg, P., Arlt, E., Briukhovetska, D., Ansari, M., Gunsel, G.G., Conlon, T.M., Wyatt, A., Wetzel, S., Teupser, D., Holdt, L.M., Ectors, F., Boekhoff, I., Boehm, U., Garcia-Anoveros, J., Saftig, P., Giera, M., Kobold, S., Schiller, H.B., Zierler, S., Gudermann, T., Wahl-Schott, C., Bracher, F., Yildirim, A.O., Biel, M., Grimm, C., 2022. Lung emphysema and impaired macrophage elastase clearance in mucolipin 3 deficient mice. Nat. Commun. 13, 318.
Su, Y., Han, W., Giraldo, C., De Li, Y., Block, E.R., 1998. Effect of cigarette smoke extract on nitric oxide synthase in pulmonary artery endothelial cells. Am. J. Respir. Cell Mol. Biol. 19, 819–825.
Sun, X., Li, Z., Wang, X., He, J., Wu, Y., 2024. Inorganic phosphate as "Bioenergetic Messenger" triggers M2-type macrophage polarization. Adv. Sci. (Weinh.) 11, e2306062.
Tang, P.C., Chung, J.Y., Xue, V.W., Xiao, J., Meng, X.M., Huang, X.R., Zhou, S., Chan, A. S., Tsang, A.C., Cheng, A.S., Lee, T.L., Leung, K.T., Lam, E.W., To, K.F., Tang, P.M., Lan, H.Y., 2022a. Smad3 promotes cancer-associated fibroblasts generation via macrophage-myofibroblast transition. Adv. Sci. (Weinh.) 9, e2101235.
Tang, X.Y., Wu, S., Wang, D., Chu, C., Hong, Y., Tao, M., Hu, H., Xu, M., Guo, X., Liu, Y., 2022b. Human organoids in basic research and clinical applications. Signal Transduct. Target. Ther. 7, 168.
Vlahos, R., 2020. FSTL-1: a new player in the prevention of emphysema. Am. J. Respir. Crit. Care Med. 201, 886–888.
Wang, C., Hyams, B., Allen, N.C., Cautivo, K., Monahan, K., Zhou, M., Dahlgren, M.W., Lizama, C.O., Matthay, M., Wolters, P., Molofsky, A.B., Peng, T., 2023. Dysregulated lung stroma drives emphysema exacerbation by potentiating resident lymphocytes to suppress an epithelial stem cell reservoir. Immunity 56 (576–591), e510.
Xia, H., Wu, Y., Zhao, J., Li, W., Lu, L., Ma, H., Cheng, C., Sun, J., Xiang, Q., Bian, T., Liu, Q., 2022. The aberrant cross-talk of epithelium-macrophages via METTL3-regulated extracellular vesicle miR-93 in smoking-induced emphysema. Cell Biol. Toxicol. 38, 167–183.
Xia, H., Wu, Y., Zhao, J., Cheng, C., Lin, J., Yang, Y., Lu, L., Xiang, Q., Bian, T., Liu, Q., 2023. N6-Methyladenosine-modified circSAV1 triggers ferroptosis in COPD through recruiting YTHDF1 to facilitate the translation of IREB2. Cell Death Differ. 30, 1293–1304.
Yang, X., Li, S., Zhao, Y., Li, S., Zhao, T., Tai, Y., Zhang, B., Wang, X., Wang, C., Chen, J., Wang, Q., Zhang, L., Xu, D., Chang, Y., Wei, W., 2019. GRK2 mediated abnormal transduction of PGE2-EP4-cAMP-CREB signaling induces the imbalance of macrophages polarization in collagen-induced arthritis mice. Cells 8.
Yoshida, M., Minagawa, S., Araya, J., Sakamoto, T., Hara, H., Tsubouchi, K., Hosaka, Y., Ichikawa, A., Saito, N., Kadota, T., Sato, N., Kurita, Y., Kobayashi, K., Ito, S., Utsumi, H., Wakui, H., Numata, T., Kaneko, Y., Mori, S., Asano, H., Yamashita, M., Odaka, M., Morikawa, T., Nakayama, K., Iwamoto, T., Imai, H., Kuwano, K., 2019. Involvement of cigarette smoke-induced epithelial cell ferroptosis in COPD pathogenesis. Nat. Commun. 10, 3145.
Zhang, Q., Wang, W., Zhou, Q., Chen, C., Yuan, W., Liu, J., Li, X., Sun, Z., 2020. Roles of circRNAs in the tumour microenvironment. Mol. Cancer 19, 14.
Zhao, J., Xia, H., Wu, Y., Lu, L., Cheng, C., Sun, J., Xiang, Q., Bian, T., Liu, Q., 2023. CircRNA_0026344 via miR-21 is involved in cigarette smoke-induced autophagy and apoptosis of alveolar epithelial cells in emphysema. Cell Biol. Toxicol. 39, 929–944.
Zhao, L., Zhang, H., Liu, X., Xue, S., Chen, D., Zou, J., Jiang, H., 2022. TGR5 deficiency activates antitumor immunity in non-small cell lung cancer via restraining M2 macrophage polarization. Acta Pharm. Sin. B 12, 787–800.